

# Testing a Mathematical Model of the Yeast Cell Cycle

Frederick R. Cross,\* Vincent Archambault, Mary Miller, and  
Martha Klovstad

The Rockefeller University, New York, New York 10021

Submitted May 25, 2001; Revised September 25, 2001; Accepted October 10, 2001  
Monitoring Editor: Mark J. Solomon

We derived novel, testable predictions from a mathematical model of the budding yeast cell cycle. A key qualitative prediction of bistability was confirmed in a strain simultaneously lacking *cdc14* and G1 cyclins. The model correctly predicted quantitative dependence of cell size on gene dosage of the G1 cyclin *CLN3*, but it incorrectly predicted strong genetic interactions between G1 cyclins and the anaphase-promoting complex specificity factor Cdh1. To provide constraints on model generation, we determined accurate concentrations for the abundance of all nine cyclins as well as the inhibitor Sic1 and the catalytic subunit Cdc28. For many of these we determined abundance throughout the cell cycle by centrifugal elutriation, in the presence or absence of Cdh1. In addition, perturbations to the Clb-kinase oscillator were introduced, and the effects on cyclin and Sic1 levels were compared between model and experiment. Reasonable agreement was obtained in many of these experiments, but significant experimental discrepancies from the model predictions were also observed. Thus, the model is a strong but incomplete attempt at a realistic representation of cell cycle control. Constraints of the sort developed here will be important in development of a truly predictive model.

## INTRODUCTION

The eukaryotic cell cycle is controlled by cyclin-dependent kinase activity, where the activity of the kinases is controlled by abundance of the positive regulatory cyclin subunits and by phosphorylation of the kinase catalytic subunit (Morgan, 1997). Cyclins are regulated transcriptionally and proteolytically; this regulation is interdigitated with control of chromosome replication and segregation (Nasmyth, 1996; Zachariae and Nasmyth, 1999) and spindle morphogenesis (Haase *et al.*, 2001).

Chen *et al.* (2000) presented a mathematical model of the budding yeast cell cycle that formulates a great deal of genetic and biochemical data, in terms of chemical kinetic rate equations. The model contains a number of simplifications. All cyclins are implicitly assumed to be nuclear (Novak *et al.*, 1998), although this is not always the case (Miller and Cross, 2000). A number of nonessential cyclins are omitted (*CLN1*, *CLB1,3,4,6*). The model lacks modeling of control of mitotic exit by the Cdc14 phosphatase and the mitotic exit network that controls it (Jaspersen *et al.*, 1998; Shou *et al.*, 1999; Visintin *et al.*, 1999; Bardin *et al.*, 2000).

An important component in the model is the delayed activation of the anaphase-promoting complex (APC) specificity factor Cdc20 due to checkpoint/surveillance mecha-

nisms dependent on chromosome replication and alignment on the metaphase spindle. Because such surveillance mechanisms are at least individually dispensable for viability (Zhao *et al.*, 1998; Alexandru *et al.*, 1999; Vallen and Cross, 1999; Bardin *et al.*, 2000), it is unlikely that a delay in Cdc20 activation due to damage surveillance is an essential component of the cell cycle oscillator.

Despite these limitations, the model implements an interesting concept of the cell cycle as an alternation of two states: a low-Clb state in which Clb inhibitors and degradation are high and a high-Clb state in which the reverse is true (Nasmyth, 1996). Well-characterized pathways are proposed to make these states self-maintaining. For example, the Sic1 inhibitor of B-type cyclin-dependent kinase activity is proteolyzed after its ubiquitination, and ubiquitination is in turn dependent on cyclin-dependent kinase phosphorylation of Sic1 (Verma *et al.*, 1997a, 1997b). Thus, the inhibitor will be degraded, and the kinase will therefore not be inhibited, if and only if the kinase starts at a high activity level. A similar pattern exists for Cdh1/Hct1 (Schwab *et al.*, 1997; Visintin *et al.*, 1998), which activates ubiquitination and subsequent proteolysis of some B-type cyclins. Phosphorylation of Cdh1 by cyclin-dependent kinases prevents its ability to cause cyclin ubiquitination by the APC (Zachariae *et al.*, 1998; Jaspersen *et al.*, 1999).

In the model, the Cln-dependent kinases drive transition from the low-Clb to the high-Clb state (in part by phosphorylating both Sic1 and Cdh1), and Cdc20 drives the reverse transition by initiating Clb proteolysis. Hysteresis is pre-

DOI: 10.1091/mbc.01-05-0265.

\* Corresponding author. E-mail address: fcross@rockvax.rockefeller.edu.

dicted in the transitions between these states, such that the forces driving the transition must push for a while before the transition occurs, making the transitions irreversible.

The model accounts for an impressive number of mutant situations (Chen *et al.*, 2000), but all of these situations were used as input information to generate the model and so were not independent confirmation. Here we derive and test new predictions from the model. The results of these studies suggest the need for more empirically based parameters for future modeling efforts. In the second part of this article we obtain absolute quantitative information on the abundance of most cell cycle regulators through the cell cycle. Such information is likely to provide constraints that will make future models significantly more realistic and may lead to the development of mathematical models usable as predictive tools for cell cycle control.

## MATERIALS AND METHODS

### Strain and Plasmid Constructions

In Figures 1–3, strains were BF264-15D background. *bck2::ARG4* strains (Epstein and Cross, 1994) were transformed with an integrating *TRP1-CLN3* plasmid containing ~3.5 kb of 5' and 1.2 kb of 3' information, targeted to *trp1* by *Bgl*III digestion or an identical plasmid lacking *CLN3*. Transformants were mated to a *cln3::URA3* strain and meiotic segregants identified with and without *BCK2*, endogenous *CLN3*, and the *CLN3* transgene. Transgene copy number was established by digestion of DNA (Holm *et al.*, 1986) from Trp+ segregants with *Bgl*III, yielding a 7.1-kb endogenous *CLN3* band and an 11.6-kb transgene band, quantitated by Southern hybridization and Phosphorimager. Ratios of transgene to endogenous signal (duplicate meiotic segregants for each initial transformant) indicate transgene copy number. A correction was required for apparently lower recovery or transfer of the 11.6-kb transgene fragment. Strains with the minimum ratio detected gave a ratio of ~0.5 rather than 1. We assume these to be single copy. This ratio was the most commonly detected (3/7), and these are stable integrants in which effectively one copy of *CLN3* is functioning, based on essentially equal cell volume of *cln3::URA3* cells containing the transgene to *CLN3* cells not containing the transgene. Therefore, to obtain *CLN3* copy number in the transgene array, we multiplied the (11.6 kb/7.1 kb) signal ratio by 2 and rounded to the nearest integer. The total *CLN3* copy number in a strain is this number, plus one for strains containing endogenous *CLN3*.

The *CLN3<sup>myc</sup>* integration vector pMM162 was constructed by moving the *Sall*-*Sac*II cassette of pMM99 (Miller and Cross, 2000) containing *CLN3* promoter driven *CLN3<sup>myc</sup>* into the *Sall*-*Sac*II site of the integration vector pRS404. This vector was targeted for integration at *CLN3* by digestion with *Eco*RI, resulting in introduction of a C-terminal Cln3-myc epitope followed by *TRP1* and untagged *CLN3*.

Protein A (PrA) tagging (W303 background) was performed by the PCR-based method (Aitchison *et al.*, 1995) using pBXAHIS5 (Wach *et al.*, 1997). Integration was verified by PCR using flanking oligonucleotides. Myc-epitope tagging was described for Cln2, Cln3, and Clb5 (Jacobson *et al.*, 2000; Miller and Cross, 2000).

The *cdh1::LEU2* (*hct1::LEU2*) allele was from W. Seufert (Schwab *et al.*, 1997) in the W303 background, and for the experiment in Figure 3 was backcrossed six times into BF264-15D. The *GALL-HA-HCT1-m11* mutant expressing unphosphorylatable Cdh1/Hct1 (Zachariae *et al.*, 1998; W303 background) was provided by M. Shirayama. (Note: the standard name for this locus according to the Stanford Saccharomyces Genome database is *CDH1*, with *HCT1* listed as a nonstandard alias; see <http://genome-www4.stanford.edu/cgi-bin/SGD/locus.pl?locus=cdh1>. We will use the standard name throughout this article, although the Hct1 name was used in Chen

### *cln1,2,3 GAL-CLN3 cdc14-1*

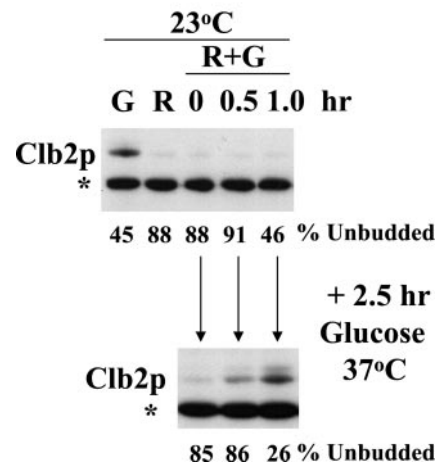


**Figure 1.** Hysteresis in the cell cycle. A strain of genotype *cln1 cln2 cln3 GAL-CLN3 cdc14-1* was grown to log phase in YEPGal (galactose medium, *GAL-CLN3* on) at 23°C and blocked due to *CLN* deficiency by incubation in YEP Raff (raffinose medium, *GAL-CLN3* off) at 23°C for 6 h. Galactose was then added to 3% final concentration to induce *GAL-CLN3*. At the indicated times after galactose addition, aliquots of the culture were removed. Some of the aliquot was immediately extracted for immunoblotting with anti-Clb2 antibody. To the rest of the aliquot glucose was added to 2% final concentration to repress *GAL-CLN3*, and the aliquot was incubated at 37°C for 2.5 h. The aliquot was then extracted for immunoblotting. The percentages of unbudded cells at the time of aliquot removal and after the 2.5-h incubation in glucose at 37°C were determined microscopically. Top: Clb2 immunoblot for cells in continuous galactose (G), after the raffinose block (R), and after the indicated amounts of time after galactose addition (R+G; all at 23°C). Bottom: Clb2 immunoblot for cells incubated in R+G for the indicated amount of time and then shifted to glucose at 37°C for 2.5 h. \*An unidentified background band used for standardizing protein loading. The percentage of unbudded cells at the time of protein harvest is indicated below the gel lanes. The top and bottom immunoblots were from the same membrane and film exposure.

*et al.* [2000] as well as in many other publications. We hope this will cause neither confusion nor offense).

### Protein Methods

9XMyc or PrA-containing DNA was cloned into *Not*I-cut pET42a (Novagen, Madison, WI), encoding GST-HIS. The PrA *Not*I fragment was obtained from pMM53, constructed by replacing the 3× HA epitope of pKL001 (Levine *et al.*, 1996) with a PCR-amplified *Not*I fragment containing PrA.

BL21-DE3 with these plasmids was grown to OD<sub>600</sub> 0.5, induced with 1 mM IPTG for 5 h and lysed by sonication in 100 mM NaH<sub>2</sub>PO<sub>4</sub>, 10 mM Tris, pH 8.0, 8 M urea, 0.5 mM PMSF, 1 μg/ml pepstatin, 1 μg/ml leupeptin, and 0.2% aprotinin. Nickel resin (QIAGEN, Santa Clarita, CA) was added to cleared lysate, rocked at room temperature for 30 min, and washed using the same buffer at pH 6.3. Fusions were eluted using the same buffer with imidazole (0.2 M), pH 4.5.

*Escherichia coli* expressing MBP-Clb2 (from P. Kaldis) was grown at 37°C in LB + 100 μg/ml ampicillin, 0.2% glucose. After 30 min at 23°C cells were induced with 0.3 mM IPTG for 6 h, suspended in ice-cold column buffer (20 mM Tris 7.5, 200 mM NaCl, 1 mM EDTA,

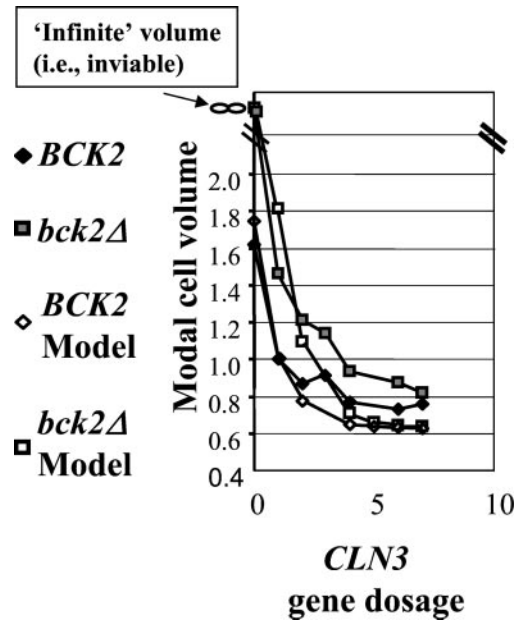


**Figure 2.** The effect of *CLN3* gene dosage on cell size control. For the model predictions, standard parameters from Chen *et al.* (2000) were used. Changes in *CLN3* gene dosage were simulated by changing the DN3 parameter. *bck2* deletion was simulated by reducing the BCK parameter to 0. The modal cell volume from the model was estimated as the midpoint between the size at birth and at cell division, relative to a wild-type value of 1. For the experimental observations, cultures of the appropriate genotype (see MATERIALS AND METHODS) were grown to log phase in YEPD, and the peak modal cell size was determined relative to a wild-type control, set to a value of 1. The total *CLN3* gene dosage was taken to be the calculated number of *CLN3* genes in the transgene array for strains that were *cln3::URA3* at the endogenous *CLN3* locus. *CLN3* gene dosage was incremented by one for strains with wild-type *CLN3* at this position.

1 mM DTT, 200  $\mu$ g/ml PMSF), frozen at  $-20^{\circ}\text{C}$  overnight, thawed on ice, and sonicated with a Misonix XL2020 sonicator microtip (setting 5, 16  $\times$  15-s bursts, 1-min rests on ice; Farmingdale, NY), centrifuged for 10 min at 9000 rpm at  $4^{\circ}\text{C}$ , added to 1 ml amylose resin (New England Biolabs, Beverly, MA), agitated  $4^{\circ}\text{C}$  for 8 h, washed three times with ice-cold column buffer, and eluted three times with 1 ml ice-cold column buffer containing 10 mM maltose.

Fusion proteins (GST-PrA, GST-Myc, and MBP-Clb2) were quantified as follows. SDS-PAGE gels of the fusions along with BSA standards were stained with Coomassie Brilliant Blue R-250 (ICN Biomedicals, Costa Mesa, CA). The predominant band in each aliquot corresponded to the purified recombinant protein. The mass corresponding to this band was estimated by comparing intensity with the BSA standards. A mass ratio for the full-length fusion protein over total protein in the lane was estimated at between 25 and 50%. Protein concentrations were assayed by a Bradford (Pierce, Rockford, IL) and a Lowry (DC Protein Assay; Bio-Rad, Hercules, CA) assay, and the protein concentrations were corrected for impurities using the ratio estimated from the gel. These values were averaged to determine the concentration of the fusion proteins.

Yeast proteins were extracted with glass bead/SDS extraction (Levine *et al.*, 1996) or NaOH/TCA extraction as follows. Pelleted cells were resuspended in 500  $\mu$ l of 1.85 N NaOH, 7.4% BME, incubated on ice for 1 h, and then precipitated with 500  $\mu$ l 50% TCA

at  $0^{\circ}\text{C}$  for 1 h. Precipitates were pelleted at 14,000 rpm at  $4^{\circ}\text{C}$  for 1 h, washed with acetone at  $-20^{\circ}\text{C}$ , and resuspended in 100  $\mu$ l 0.5 M Tris, 5% SDS by sonicating. One hundred microliters of 75% glycerol, 250 mM DTT, and 0.05% bromphenol blue were added, and samples were incubated at  $95^{\circ}\text{C}$  for 15 min and centrifuged to pellet debris. For data in Tables 1 and 2, both methods were used as indicated. For other experiments, the glass bead method was used. These methods were compared in parallel and found to be approximately equally efficient at cell breakage and protein yields (our unpublished data).

For quantitation, diploid strains expressing PrA fusions were grown in YEPD to  $1-2 \times 10^7$  cells/ml. Triplicate hemocytometer cell counts were used to determine number of cell equivalents of protein analyzed. Serial dilutions of cell extracts and of the recombinant GST-PrA were made in carrier cell extracts obtained from control untagged cultures. Samples were run on 5–20% acrylamide gels and analyzed by Western blot on the same piece of membrane. PrA detection was with rabbit IgG (ICN) followed by donkey anti-rabbit, HRP-coupled antibody (Amersham, Arlington Heights, IL), with chemiluminescent detection. Films with exposures in the linear range were analyzed for signal intensities after background subtraction, using a digital camera and pixel quantifying software (Alpha Innotech, San Leandro, CA). From the dilution of standard and its concentration, a conversion for signal intensity to number of molecules was determined, yielding an estimate for the number of copies per cell (see Figure 4 legend). For myc-tagged proteins, GST-myc standard and polyclonal anti-Myc antibody were used (Santa Cruz Biotechnology, Santa Cruz, CA). For untagged Clb2, the standard was MBP-Clb2, and the dilutions were made in extract from a *clb2* deletion strain. Blots were probed with anti-Clb2 antibody (Santa Cruz).

Densitometry was used similarly for quantifying results from the elutriation experiments. Because of the large number of samples, the serial dilution strategy was not used, but the exposures were in the linear range of detection. In these experiments, signal from the PrA fusion was standardized by determination of Pgc1 protein levels in the fractions, using anti-Pgc1 antibody (Molecular Probes, Eugene, OR) in parallel immunoblots.

### Competition Growth Assay

Fresh stationary phase plate stocks of variously marked gene disruptions were mixed in approximately equal proportions in water. The suspension was streaked out on nonselective YEPD solid medium, and the suspension was also inoculated at  $\sim 200$  cells/ml in YEPD, and flasks were incubated with shaking for 2 d at  $30^{\circ}\text{C}$ , to stationary phase. The frequencies of prototrophs for the disruption markers before and after culture growth were determined by plating. The selective disadvantage in this one-step growth regimen was determined as follows:  $T_m/T_w = \ln(I * f_{Wend}/f_{Wbeg})/\ln(I * f_{Mend}/f_{Mbeg})$ , where  $I$  is the fold increase in cell number through the experiment (500,000),  $f_{Wend}$  is the frequency of wild types at end,  $f_{Wbeg}$  is the frequency of wild types at beginning; and  $f_{Mend}$  and  $f_{Mbeg}$  are frequencies for the mutants. This parameter will reflect differential growth rates in exponential growth, if time of exit and entry into stationary phase and differential survival in the stationary phase are ignored. We have not evaluated the latter possibilities.

As controls for the disruptions, we tested W303 strains that were *HIS3*, *LEU2*, *TRP1*, or *URA3* in competition with normal W303. The final calculated selective disadvantage due to the cyclin disruption is the disadvantage of the disrupted strain compared with wild type, divided by the selective advantage of the appropriate control strain compared with the reference wild type.

### Elutriation

Elutriation was carried out in a Beckman J6 M elutriating centrifuge (40-ml chamber) at  $4^{\circ}\text{C}$  and 2700 rpm. One-liter cultures in YEPD medium ( $\text{OD}_{660}$ , 1.0) were collected by filtration, resuspended in 100

**A.**

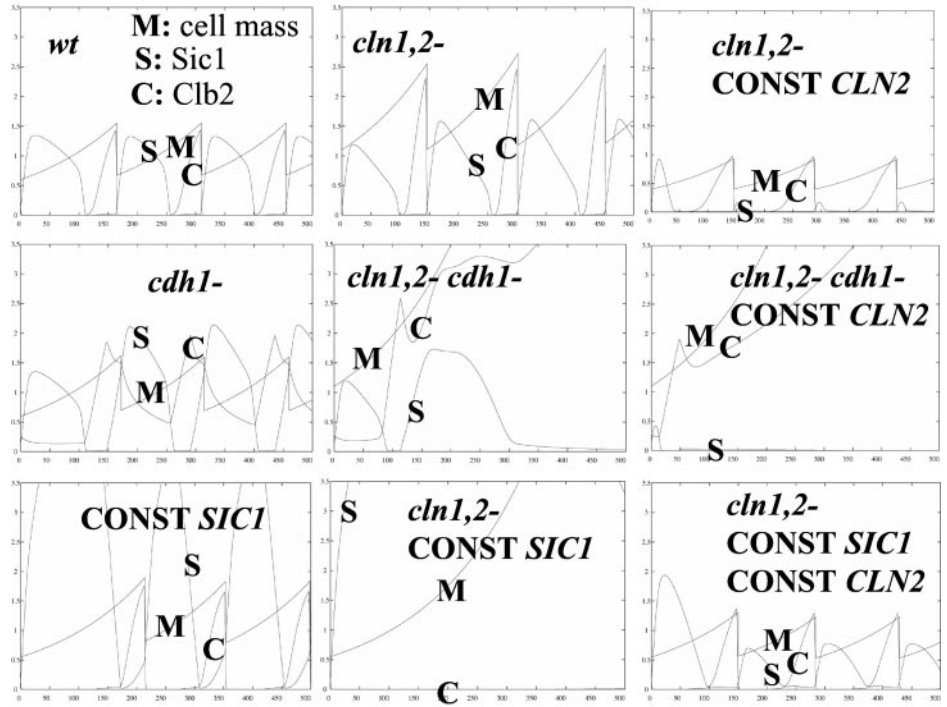


**Figure 3.** Interaction between G1 cyclins and mitotic regulators Sic1 and Cdh1. (A) Model predictions for various genotypes. Parameters: M, cell mass; C, Clb2 levels; S, Sic1 levels. Standard parameters from (Chen *et al.*, 2000) were used throughout, except for the following changes to model the mutants: *cln1,2-*:  $k_{sn2''} = 0$ ; *CONST CLN2*:  $k_{sn2'} = 0.05$ ,  $k_{sn2''} = 0$ ; *cdh1-*:  $k_{db2''} = 0.01$ ; *CONST SIC1*:  $k_{sc1'} = 0.1$ ,  $k_{sc1''} = 0.1$ . The model predicts lethality (cell cycle arrest and failure of cell division) in the *cln1,2 cdh1*, the *CONST CLN2 cdh1* (with or without *CONST SIC1*), and the *cln1,2-CONST SIC1* (with or without *CDH1*) situations. The *CONST CLN2 cdh1 CONST SIC1* simulation (not shown) is similar to the *CONST CLN2 cdh1* simulation. The *cln1,2-CONST SIC1 cdh1* simulation differs from the *cln1,2-CONST SIC1* simulation, because Clb2 levels ultimately rise because of *cdh1* deletion, but in both cases inviability is predicted. (B) Genetic test of the predictions in A. Strains (BF264-15D background) of the indicated genotypes were constructed by tetrad analysis, using *GAL-SIC1/URA3* and *GAL-CLN2/TRP1* cassettes and using a *cdh1::LEU2* deletion (Schwab *et al.*, 1997) backcrossed five times into the BF264-15D background. All strains were *cln1 cln2 CLN3*. *cln1 cln2 CLN3* corresponds to absence of Cln2 in the model, and *cdh1::LEU2* corresponds to absence of Cdh1 (called Hct1 in Chen *et al.*, 2000) in the model. The presence of the *GAL-SIC1* and *GAL-CLN2* cassettes corresponds to *CONST SIC1* and *CONST CLN2*, respectively. Tenfold serial dilutions of cultures of strains of each genotype, grown to stationary phase in YEPD, were spotted on YEPD or YEPGal plates and grown at 30°C for 2 and 3 d, respectively. Another set of strains of these genotypes behaved identically. *CLN1,2* controls (wild type, *cdh1*, and *GAL-SIC1*) are not shown here but all are viable under these conditions (our unpublished data). The model predicts lethality due to *cln1 cln2 cdh1* (YEPD plates, all *cdh1-* strains, 2nd, 4th, 6th, 8th rows), but this is not observed. It also predicts lethality due to *cln1 cln2 cdh1 GAL-CLN2* (YEPGal plates, 4th row), but this is not observed. The model correctly predicts lethality due to constitutive Sic1 expression in the absence of *cln1,2* and its rescue by constitutive *CLN2*, in the presence or absence of *cdh1* (YEPGal plates, 3rd, 4th, 7th, and 8th rows).

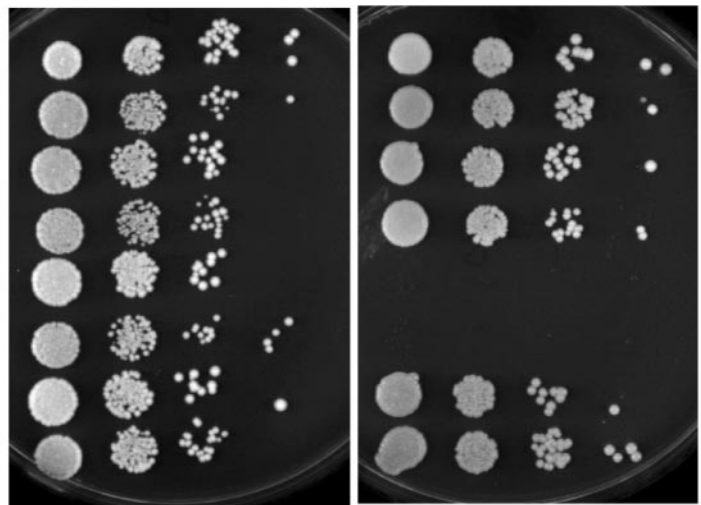
**B.**

<i>GAL1::SIC1</i>	<i>GAL1::CLN2</i>	<i>CDH1</i>
-	-	+
-	-	-
-	+	+
-	+	-
+	-	+
+	-	-
+	+	+
+	+	-

All strains are *cln1 cln2 CLN3*

YEPD

YEPGal



ml of 0°C water, sonicated three times for 1 min at maximum microtip power in a Misonix XL2020 sonicator, and loaded on the elutriating rotor. Four hundred-milliliter fractions of increasing cell volume were harvested by sequential 10% increments in pump speed, with 0°C water in the pump reservoir. Cell volume was determined using a Coulter Channelyzer calibrated with 68 fl latex beads (Coulter, Hialeah, FL).

### Computer Modeling

The WinPP program (<ftp://ftp.math.pitt.edu/pub/bardware/winpp.zip>, by Bard Ermentrout; see also <http://www.math.pitt.edu/~bard/xpp/xpp.html>) was run with a file provided by Kathy Chen that implemented the equation set in Chen *et al.* (2000). *CLN3* gene dosage was varied using the *Dn3* parameter. *bck2* deletion was simulated by setting *BCK2* to zero. *CDH1* deletion was simulated by setting *kdb2*" to 0.01. To simulate *GAL* promoter driven expression, it was assumed that constitutive expression was equal to peak regulated expression of the endogenous gene (the results of the simulations were not very sensitive to this parameter). To simulate *GAL-CLB2db*, it was assumed that neither *Cdc20*-dependent nor *Cdh1*-dependent degradation could operate ( $kdb2'' = 0.01$ ,  $kdb2p = 0$ ). To model *GAL-HCT1-m11* (unregulated *Cdh1*), *GAL* promoter expression was neglected, because *CDH1* expression is not considered in the model. Instead the nonphosphorylatable status of the mutant *Cdh1* encoded by this construct was reflected by setting *kit1*" to zero, eliminating the effect of *Cdk* phosphorylation.

## RESULTS

### Hysteresis: Is the Cell Cycle Characterized by Bistability?

A central aspect of the model derives from the bistability concept (Nasmyth, 1996), in which the cell cycle is considered as an alternation between two stable self-maintaining states, one in which *Clb* kinase is low (G1) and one in which *Clb* kinase is high (S/M). The components in the model causing switching between the two states are the *Cln* kinases for low-to-high and *Cdc20* for high-to-low. The *Cln* kinases switch from the low to the high state by phosphorylating *Sic1* and *Cdh1*, allowing accumulation of *Clb* kinases. *Clb* kinases can subsequently maintain the high state by continuing *Sic1* and *Cdh1* phosphorylation. *Cln* kinases can reverse the low state because they are immune to *Sic1* and *Cdh1* regulation, but once the *Clb* kinases are high, *Cln* kinases are dispensable (and indeed are predicted to be deleterious; see below). Conversely, *Cdc20* activates the high-to-low transition by inducing degradation of *Clb5* and initial degradation of *Clb2*; once *Clb* kinases have been pushed below a threshold level, *Sic1* and *Cdh1* phosphorylation become inefficient, and they then take over from *Cdc20* to push *Clb* kinase activity to a very low level. At this point *Cdc20* is no longer needed to maintain the low-*Clb* kinase state.

The role of *Cdc20* in the model is more limited than current information indicates. *Cdc20* not only leads to degradation of *Clb2*, but also to degradation of *Pds1*, and *Pds1* is thought to inhibit release of the *Cdc14* phosphatase from the nucleolus (see INTRODUCTION). *Cdc14* is thought to dephosphorylate and hence activate *Cdh1* and *Sic1*. For purposes of this discussion, because the available model does not include *Cdc14* and its associated regulatory machinery, we can consider *Cdc20* as a component that somehow encompasses both *Cdc20* and *Cdc14* activities, and these jointly drive *Clb* kinase from the high to the low state.

The model thus contains initiator activities (*Cln* kinases, primarily *Cln2* in the model) and terminator activities (*Cdc20*, *Cdc14*, *et al.*; *Cdc20* in the model). These initiator and terminator activities antagonize each other with respect to activation or inactivation of *Cdh1* and *Sic1*, which are the main final enforcers of the low-*Clb* state. Intriguingly, simultaneous absence of initiator and terminator activities does not result in a unique predicted final outcome; rather, hysteresis is predicted. "Hysteresis occurs in systems with multiple steady states and refers to the fact that the observed state of the system depends not only on its parameter values but also on its history (how the system is prepared)" (Novak *et al.*, 1998). Thus, if the neutral situation lacking initiator and terminator is encountered from a prior history of a low-*Clb* state, this state will be maintained indefinitely; conversely, encountering neutral coming from the high-*Clb* state means that the high-*Clb* state will be maintained. This formulation makes the prediction that a third steady state, with intermediate values of *Clb*-dependent kinases, is mathematically possible but unstable.

To try to experimentally realize the neutral state lacking both initiator and terminator, we constructed a strain of the genotype *cln1 cln2 cln3 GAL-CLN3 cdc14-1*. The strain is viable on galactose medium at 23°C, because galactose provides *CLN* function by keeping *GAL-CLN3* on, and the *cdc14-1* temperature-sensitive allele functions at 23°C. The strain is inviable at 37°C on galactose and is inviable without galactose at any temperature. Glucose medium at 37°C is the experimental approximation of the neutral state lacking initiator and terminator simultaneously. What is the phenotype of this strain in this neutral condition, and does this phenotype indeed depend on the prior history of the culture?

We blocked the strain in G1 by *CLN* deprivation, by turning off *GAL-CLN3* by incubation in raffinose medium at 23°C for 6 h. Under these conditions ~90% of the cells were unbudded (a morphological marker of the pre-Start state; Cross, 1995), and *Clb2* protein in the culture was very low (Figure 1). We then induced *GAL-CLN3* transcription with galactose. At intervals we removed aliquots of the culture, added glucose to block further *GAL-CLN3* transcription, and shifted to 37°C for 2.5 h to inactivate *cdc14-1* (*CLN3* RNA and functional *Cln3* protein disappear within minutes of *GAL-CLN3* shutoff; Cross, 1990; Tyers *et al.*, 1992; Cross and Blake, 1993). The aliquots were then analyzed for percentage of unbudded cells and *Clb2* levels. The results were consistent with the bistability prediction. Shifting the culture to 37°C + glucose without prior galactose addition (our unpublished data) or immediately after galactose addition (time zero) resulted in stable retention of the low-*Clb* state, and cells did not bud in the 2.5-h incubation in 37°C + glucose. In contrast, incubation in galactose at 23°C for 1 h before shift to 37°C + glucose resulted in acquisition of a significant level of *Clb2* at the end of the 2.5-h 37°C + glucose incubation, with most cells arrested in the characteristic large-budded morphology observed with *cdc14-1* arrest (Figure 1). This was so even though before the shift, *Clb2* protein levels were low. These results indicate that the *cln1,2,3* arrest does not require *CDC14* function for its maintenance, and the *cdc14-1* arrest does not require *CLN* function for its maintenance. The phenotype resulting from simultaneous absence of *CDC14* and *CLN* function depends on the prior history of the system, and a relatively short exposure to *CLN* function is

sufficient to commit the system to later entrance into the high-Clb state. In the absence of initiator or terminator, the system can reside in either of two states (high- or low-Clb), and which state the system adopts depends on its prior history.

Thus, Cdc14 activity is not required for maintenance of G1 arrest with low-Clb2 levels. In contrast, Cdh1 and Sic1, which are activated by Cdc14-dependent dephosphorylation, are required for maintenance of low-Clb2 G1 blocks due to *cln* deprivation (Tyers, 1996) or  $\alpha$ -factor treatment (Schwab *et al.*, 1997). Similarly, we have observed that *cln*-deficient *cdh1* mutants are inviable but arrest in glucose medium with high Clb2 levels (our unpublished data). APC activity (presumably Cdh1-dependent) is also required for maintenance of an  $\alpha$ -factor G1 block (Irniger and Nasmyth, 1997). This distinction between activities (such as Cdc14) required to enter a new state and activities (such as Cdh1 and Sic1) required to maintain the state is expected, based on the bistability hypothesis (Nasmyth, 1996; Chen *et al.*, 2000).

### Control of Cell Cycle Start by CLN3

In the model of Chen *et al.* (2000), cell cycle initiation or "Start" is coupled to cell size by the following mechanism. The Cln3 G1 cyclin is assumed to accumulate in total cellular abundance in parallel to total cell mass. It is assumed to concentrate in the nucleus (or in principle any cell compartment of constant volume) so that as its cellular abundance increases, its nuclear concentration increases. Past a certain threshold level it triggers G1/S transcription by activating SBF/MBF (Koch and Nasmyth, 1994), turning on the more downstream-acting G1 cyclins Cln1 and Cln2 along with other genes. Consistent with this model, we found recently that Cln3 does indeed accumulate in the nucleus. Also, moving Cln3 from the nucleus to the cytoplasm significantly reduces its function (Miller and Cross, 2000; Miller and Cross, submitted).

In the simplest version of the idea that cells read their size based on Cln3 nuclear abundance, one might expect that doubling Cln3 levels should result in cells reading their size as twice the actual size, thus halving the cell volume at which Start occurs. In fact, the cell volume response to doubling *CLN3* gene dosage is much more modest (Nash *et al.*, 1988; Cross, 1989; Figure 2). The model primarily accounts for this using the properties of Bck2, which acts genetically as a parallel system to Cln3 activating SBF/MBF-regulated genes (Epstein and Cross, 1994; Di Como *et al.*, 1995). In the absence of Bck2, Cln3 becomes essential, and in the absence of both Cln3 and Bck2, SBF/MBF-regulated genes are expressed at very low levels (Epstein and Cross, 1994; Di Como *et al.*, 1995). The presence of the *BCK2* gene provides backup and blunts the response to *CLN3* gene dosage. Therefore, according to the model, deleting *BCK2* should result in highly elevated responsiveness of cell size to *CLN3* gene dosage.

To test this idea, we constructed a series of strains with or without *BCK2*, in which the endogenous *CLN3* gene was either present or absent and additionally containing ectopic copies of the *CLN3* gene inserted at the *TRP1* locus. A 6.2-kb chromosomal segment containing *CLN3* was stably integrated at *trp1* in one or multiple copies (quantitated by Southern hybridization). The size of the segment makes it likely that expression levels will be little affected by the site

or copy number of integration. Indeed, we observed a similar cell volume in *cln3::URA3* strains containing a single-copy *CLN3* transgene to the cell volume of wild-type cells (our unpublished data), whereas *CLN3+* strains containing a single-copy transgene or *cln3::URA3* strains containing multiple-copy transgenes were smaller than wild type (Figure 2).

Predictions from the model for approximate modal cell volume were taken as the midpoint between predicted birth size and division size, relative to wild type. Modal cell volumes for the constructed strain set were determined by electronic cell volume measurements, relative to wild type. A reasonable correspondence between model and experiment was observed in the *BCK2* and *bck2* backgrounds (Figure 2). A minor difference may be that the model predicts a more extreme response to *CLN3* dosage than was actually observed; thus the size control system (with or without *BCK2*) may be more robust with respect to these genetic perturbations than predicted. (It is also possible that the effects of *CLN3* gene dosage saturate at higher levels due to limitation of some other factor). It is important to note that although limited information on the relationship between *CLN3* gene dosage and cell size was used as input information in formulating the model, these data were all in a *BCK2* background. Therefore, the *bck2* results presented here are independent confirmation of the model.

An interesting feature of *CLN3* expression is that it is under moderate cell cycle regulation, with RNA expression peaking in late M/early G1 (McInerney *et al.*, 1997). This feature is not implemented in the model, and it is unclear how its implementation would affect these size control predictions.

### Predicted Interactions between G1 Cyclin Function and Mitotic Regulators Sic1 and Cdh1

The model makes critical use of Cln2 as an initiator activity to drive cells from a low-Clb to a high-Clb state, because Cln2-dependent phosphorylation is assumed to be able to reverse two independent controls that reinforce the low-Clb state, Sic1 stability, and Cdh1 function. Cdh1 (Hct1 in the model; see MATERIALS AND METHODS for a note on nomenclature) is thought to control Clb2 degradation in mitotic exit, and most specifically in the G1, low-Clb state (Schwab *et al.*, 1997; Visintin *et al.*, 1998). Cdh1 is dispensable for viability, presumably because Sic1 is sufficient to control Clb kinase levels, as evidenced by specific lethality of *cdh1 sic1* double mutants (Schwab *et al.*, 1997; Visintin *et al.*, 1998).

*SIC1* expression is also transcriptionally controlled (Knapp *et al.*, 1996; Toyn *et al.*, 1996), and this is implemented in the model. This control is helpful but not essential in the model: making *SIC1* transcription constitutive at the level of peak regulated expression is not lethal (Figure 3A, CONST *SIC1*), because first Cln2 and later Clb5 and Clb2 can keep Sic1 protein levels low. Deleting *CLN2* in the model results in lethality of constitutive *SIC1* expression (*cln1,2-CONST SIC1*), as has been observed experimentally (*cln1 cln2 GAL-SIC1* strains are inviable; Tyers, 1996).

*CLN2* is turned off transcriptionally by Clb2 (Amon *et al.*, 1993; Koch *et al.*, 1996). This regulation is implemented in the model, where it is helpful but not essential: constitutive *CLN2* expression (at the level of peak regulated Cln2 expression) is not predicted to be lethal (CONST *CLN2*). Constitu-

tive *CLN2* expression in the *cln1,2* background is predicted to rescue inviability due to constitutive *SIC1* expression (CONST *CLN2*, CONST *SIC1*).

In contrast, the model predicts that constitutive *CLN2* expression should be lethal in the absence of *Cdh1*, presumably because then the cell becomes highly sensitive to the ability of even low-level *Cln2* to destabilize *Sic1* by phosphorylation (CONST *CLN2 cdh1*-). Interestingly, at the other extreme, the model predicts that complete absence of *Cln2* should be lethal in the absence of *Cdh1* (*cln1,2-cdh1*-). This lethality is predicted because in the absence of *Cln2*, cell cycle Start occurs at abnormally large size. Therefore, when *Clb2* cyclin accumulates, it is driven by the large cell mass to levels that require the presumed catalytic activity of *Cdh1* for effective *Clb2* disposal. Thus, the model makes two predictions: that *Cln2* constitutive expression should be lethal in the absence of *Cdh1* and that simultaneous removal of *Cln2* and *Cdh1* should also be lethal. In these simulations, constitutive *Cln2* expression from the *GAL* promoter is set to be equal to peak expression of the endogenous gene, but the results are not very sensitive to this level (our unpublished data).

To test these predicted interactions, we constructed a diploid with the genotype *cdh1::LEU2/CDH1 GAL1::CLN2::TRP1/trp1 GAL1::SIC1::URA3/ura3 cln1/cln1 cln2/cln2*. Segregants of this diploid were tested for viability on glucose or galactose medium (where the *GAL*-controlled cassettes were off or on). As expected, *GAL-SIC1* expression resulted in inviability in the *cln1,2* background (Tyers, 1996), and this inviability was rescued by *GAL-CLN2* expression (Figure 3B, +*GAL-SIC1*, vs. +*GAL-SIC1* +*GAL-CLN2*). These observations meet the expectation of the model (Figure 3A, *cln1,2-CONST SIC1* vs. *cln1,2-CONST SIC1 CONST CLN2*). In contrast to the expectations of the model, this *CLN2* overexpression cassette, which effectively rescued inviability due to *GAL-SIC1*, did not cause lethality in the absence of *CDH1* (Figure 3A, *cln1,2-cdh1-CONST CLN2*; Figure 3B, +*GAL-CLN2*, +*GAL-CDH1*). Also, there was no reduction of viability of the *cln1 cln2* segregants (without *GAL1::CLN2* or *GAL1::SIC1* expression) due to *cdh1* deletion, although the model predicts absolute inviability of *cdh1 cln1 cln2* strains (Figure 3A, *cln1,2 cdh1*-; Figure 3B, all *cdh1*- strains on glucose medium).

One possible explanation for the viability of *GAL-CLN2 cdh1* strains, that *Cln2* expressed late in the cell cycle is unable to form an active complex with *Cdc28* kinase, is contradicted by previous experimental evidence (Amon *et al.*, 1993).

Fiddling with the parameter set for the model can remedy some of these incorrect predictions. For example, increasing the rate of *Sic1* expression threefold rescues lethality due to constitutive *Cln2* expression in the absence of *Cdh1*, but does not rescue inviability due to lack of *Cln2* and *Cdh1*. Lowering *Clb2* synthesis rates twofold rescues inviability due to lack of *Cln2* and *Cdh1*, but does not rescue lethality due to constitutive *Cln2* in the absence of *Cdh1*. These two changes in the parameter set work essentially by increasing the *Sic1/Clb2* ratio and thus help the model to inactivate *Clb2* kinase even in the absence of *Cdh1*-mediated *Clb2* degradation. Alternatively, increasing the ability of *Cdc20* to degrade *Clb2* (by increasing *kdb2p* from 0.05 to 0.5) rescues inviability due to lack of *Cdh1* combined with either *Cln2* overexpression or *Cln2* absence. This change works by re-

ducing the importance of *Cdh1* in controlling *Clb2* abundance. A related solution (K. Chen and J. Tyson, personal communication) is to increase *Sic1* expression twofold and also to increase *Cdc20*-dependent *Clb2* degradation fourfold. Possible empirical justification for increasing *Cdc20*-dependent *Clb2* degradation are discussed below (see DISCUSSION), but the case is still unclear.

These findings emphasize a significant problem with the modeling approach: in the absence of empirical constraints on parameters, one is free to propose any parameters that fit the available data. Therefore, it appears likely that before this or any future model can be forcefully tested, more of the parameters need to be based on empirical data. An initial step toward accumulating a suitable data set is the subject of the remainder of this article.

### Quantitative Analysis of Abundance of Cell Cycle Regulators

There is a large amount of information available on regulation of abundance of cyclins through the yeast cell cycle (summarized in Chen *et al.*, 2000). A nearly universal deficit in this data set is that one can almost never compare quantities of one cyclin to another, and absolute abundance of these proteins have never been determined. The work of Tyers on the G1 cyclins (Tyers *et al.*, 1993) is an exception to the first point. Tyers *et al.* tagged the three *CLN* cyclins identically with the HA epitope tag, such that after immunoprecipitation and Western analysis, the abundance of the three tagged cyclins could be compared with each other. A problem with this analysis was that detection of *Cln3* (clearly the least abundant) was so low that the exact reduction in its abundance could not be determined. A related problem was that for some of Tyers' experiments, immunoprecipitation was required before Western analysis, with unknown losses in this step.

### PrA Tagging

We constructed strains in which endogenous cyclin genes were C-terminally tagged with protein A, with expression from the endogenous promoter and chromosomal location. It is important to confirm that any epitope tag addition does not significantly affect function of the tagged protein. To address this, we performed a range of tests on most of the PrA-tagged genes.

*Cdc28-PrA*-expressing haploids were viable; because *Cdc28* is essential, the PrA tag cannot have inactivated function. All the PrA-tagged haploid strains had essentially normal FACS profiles (our unpublished data). In contrast, *clb5*, *clb2*, or *sic1* deleted strains have increased proportions of cells between 1 and 2C DNA content (*clb5*; Epstein and Cross, 1992) or increased proportions of 2C DNA content cells (*sic1*, *clb2*; Surana *et al.*, 1991; Schwob *et al.*, 1994). This indicates approximately normal function of the tagged *Cdc28*, *Clb5*, *Clb2*, and *Sic1*. *sic1::HIS3/+* diploids and *sic1::HIS3/SIC1-PrA* diploids had FACS profiles indistinguishable from wild type, in contrast to the defective profile of *sic1::HIS3* homozygous diploids (with few or no 1C DNA content cells). This indicates full function of the PrA-tagged *Sic1* even under conditions potentially limiting for *Sic1* (our unpublished data).

*clb3* and *clb1* inactivation do not have an identified phenotype. Therefore, we tested the PrA-tagged versions by crossing them to a *clb2::LEU2* strain, because *clb1 clb2* and *clb2 clb3* double mutants are inviable (Fitch *et al.*, 1992). In parallel we crossed a *clb1::URA3* and a *clb3::TRP1* strain to the *clb2::LEU2* strain. In tetrad analysis from these diploids, we confirmed inviability of *clb1 clb2* and *clb2 clb3* double mutants. In contrast, *CLB1-PrA clb2* and *CLB3-PrA clb2* double mutants were recovered at the expected frequency and did not have a significant slow-growth phenotype compared with *clb2* single mutants, although this was not evaluated quantitatively (our unpublished data).

*clb2* deletion results in a significant delay in the cell cycle after DNA replication (Surana *et al.*, 1991), and *CLB1* and *CLB3* are both partially redundant with *CLB2* (Fitch *et al.*, 1992). Therefore, if PrA-tagged *Clb1* or *Clb3* were reduced in function, then *clb2 CLB1-PrA* or *clb2 CLB3-PrA* strains might be expected to have an exacerbated postreplicative delay relative to that in *clb2 CLB1 CLB3* strains. We compared the phenotypes of *clb2 CLB1-PrA* and *clb2 CLB3-PrA* strains to *clb2 CLB1 CLB3* strains by FACS analysis and observed little difference, although the *clb2 CLB3-PrA* strains may have had a moderate decrease in the proportion of 1C cells compared with *clb2 CLB1 CLB3* strains (our unpublished data). Overall, these data indicate that the tagged *Clb1* and *Clb3* have a significant degree of biological function.

*clb5 CLB6* strains exhibit a lengthened period of DNA replication and a compensating decrease in the population of cells with 1C DNA content. Deletion of *clb6* in the *clb5* background results in a long delay before replication and a large increase in the population of cells with 1C DNA content (Epstein and Cross, 1992; Schwob and Nasmyth, 1993). This is due to activation of early but not late origins of replication by *Clb6* in the absence of *Clb5*; when both *Clb5* and *Clb6* are deleted, neither class of origins is activated until *Clb1,2,3,4* are activated later in the cell cycle (Donaldson *et al.*, 1998). We therefore tested *CLB6-PrA* in a *clb5* background by FACS analysis, to test the ability of *CLB6-PrA* to promote early origin activation. We found that *clb5 CLB6-PrA* strains had FACS profiles similar to *clb5 CLB6* strains, lacking the strong accumulation of 1C DNA content cells seen in *clb5 clb6* strains, suggesting significant ability of *Clb6-PrA* to activate early origins of replication (our unpublished data). The population of cells with 1C DNA content was slightly increased in *clb5 CLB6-PrA* strains compared with *clb5 CLB6* strains, suggesting a moderate reduction of *Clb6-PrA* function compared with *Clb6*.

*cln3* disruption results in a cell volume increase of at least 50% (Cross, 1988; Nash *et al.*, 1988), while *CLN3-PrA* strains exhibited at most a 10% increase in cell volume (our unpublished data). *CLN3-PrA* also rescued *cln1 cln2 cln3* inviability about as well as did wild-type *CLN3* (the latter assay was performed using low-copy-number plasmids, expressing *CLN3* or *CLN3-PrA* from the *CLN3* promoter; our unpublished data). Thus, *Cln3-PrA* was functional.

As a further functional test, we tested *Cln2-PrA*, *Clb5-PrA*, and *Clb2-PrA* for binding to *Cdc28* by constructing strains expressing both the PrA-tagged cyclin and HA-tagged *Cdc28* and purifying the PrA-tagged cyclin on IgG-agarose. Although the result was not quantitated, all three cyclins bound *Cdc28*-HA roughly in accordance with the abundance of the cyclin (our unpublished data). For all nine

cyclins, we also were able to recover IgG-agarose-purified histone H1 kinase activity, indicating that the tagged cyclins were able to activate enzymatic activity of bound *Cdc28*.

Thus, the PrA fusions generally exhibit significant biological and biochemical function and in most cases function similarly to the untagged wild-type genes. Moderate reductions in function cannot be ruled out in most cases, and this leads to a caveat in the use of the tagged proteins for quantitation. An additional subtle caveat could be that if the PrA addition simultaneously weakens biological function but increases protein stability, the net effect could be to hide the loss of activity, while confounding the quantitative measurements of protein abundance.

### Average Copies per Cell in Asynchronous Culture

To determine copies per cell of the PrA-tagged proteins, we used the following procedure. We produced recombinant His-GST-PrA fusions in *E. coli*, purified the fusion on nickel beads, and quantitated the yield. We then performed serial dilutions of the recombinant protein and compared the signal obtained to that from serial dilutions of yeast protein extracts from known numbers of yeast cells. We used dilutions yielding signal in a linear range of detection using digital camera detection from exposed film (Figure 4). The results of this quantitation are presented in Table 1.

### Validation of the Quantitation

As an independent test of our data set, we constructed a recombinant GST-myc standard and quantitated myc-tagged *Cln2*, *Cln3*, and *Clb5* (Table 2). As a second independent test of our data set, we compared the abundance of endogenous *Clb2* to recombinant standard MBP-*Clb2*, using anti-*Clb2* antibody (Table 2). These independent comparisons agree with the PrA data set, within a factor of two or three. Given the number of experimental manipulations and calculations involved, we consider this agreement reasonable.

We have been able to find only one literature value to compare with our data: for *Cdc28*, 10 ng/10<sup>7</sup> haploid cells (Funakoshi *et al.*, 1997), translating to 16,000 copies per haploid cell. We calculate 12,000 copies per diploid cell (Table 1). Diploids have two copies of the *Cdc28* gene and are about twice as big as haploids. One might therefore expect to find twice as much *Cdc28* in diploid cells (although a systematic examination of the consequences of ploidy changes on individual protein levels has not been carried out to our knowledge). Thus, our estimate is in a similar range to the published one, although probably a few-fold lower.

Cells simultaneously expressing *Clb2* and *Clb5* C-terminally tagged with an HA epitope, from the endogenous promoters, show a moderate (although unquantitated) excess of *Clb2* over *Clb5* (Schwab *et al.*, 1997), consistent with our results (Tables 1 and 2).

The approximately twofold difference between *Cln2* and *Cln1* levels that we detect is slightly greater than might be expected, based on the nearly identical levels of *Cln1*- and *Cln2*-associated kinase activity reported previously using HA-tagged cyclins (Tyers *et al.*, 1993). Tyers *et al.* (1993) reported a 200-fold difference between *Cln2*-associated and *Cln3*-associated kinase activity, compared with a 15-fold

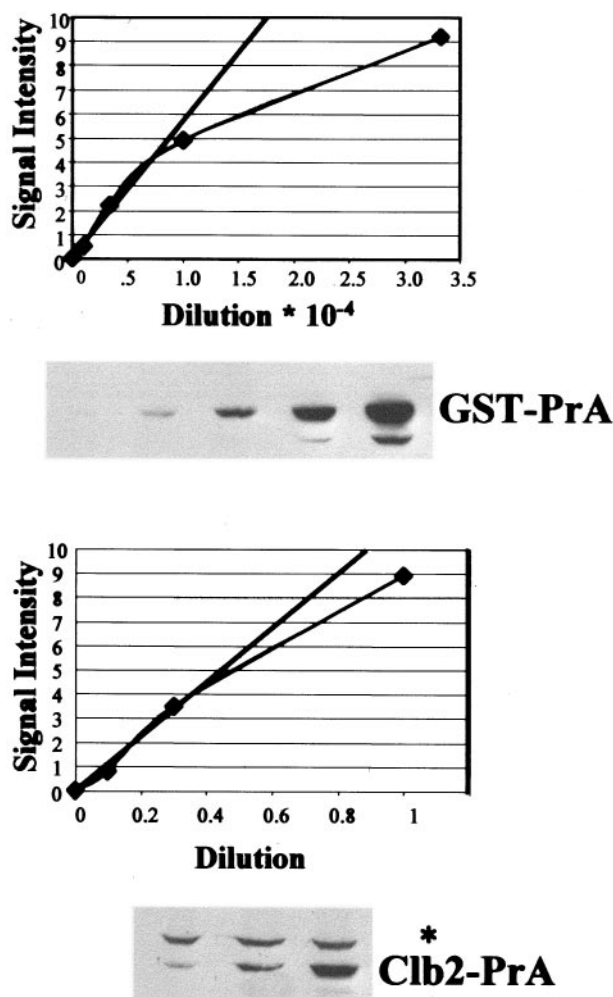


**Figure 4.** Method of quantitation: sample data for Clb2-PrA. To estimate the number of copies of a PrA fusion per yeast cell, three-fold serial dilutions of the GST-PrA standard and of the cell extract from the tagged strain were made in wild-type (untagged) carrier cell extract as described in MATERIALS AND METHODS. SDS-PAGE followed by Western blot analysis was performed with these samples. In addition to the PrA fusion protein band, all blots generated a band at ~115 kDa (asterisk), derived from the carrier wild-type cell extract. Signal intensities were plotted against dilution factors and points were chosen in the linear parts of the curve (straight line in the figure) for the calculations described in MATERIALS AND METHODS. The points in the graph correspond to the densitometric quantitation of the bands in the autoradiograph. In this example, the middle lane on the GST-PrA gel was determined to contain  $1.4 \times 10^9$  molecules of GST-PrA based on quantitation of the standard and the dilution factor, and it gave a signal intensity of 2.2, in the linear range of detection. The middle lane of the Clb2-PrA gel derived from  $4 \times 10^6$  yeast cells and gave a signal intensity of 3.5, also in the linear range of detection. The calculated Clb2-PrA/cell from this example is then  $(3.5/2.2) \times 1.4 \times 10^9$  molecules/ $4 \times 10^6$  cells = 557 molecules/cell. Because the strain analyzed was a heterozygous diploid, this number is doubled to give 1114 molecules/cell. Numerous independent determinations of this type (each representing a different protein extraction and quantitation) were averaged to yield the final numbers in Table 1.

**Table 1.** Quantitation of cyclins, Sic1, and Cdc28

Protein A-tagged protein	Copies per diploid cell (asynchronous)
Cln1	995 $\pm$ 231 (4)
Cln2	2011 $\pm$ 504 (5)
Cln3	216 $\pm$ 44 (6)
Clb1	497 $\pm$ 146 (4)
Clb2	1128 $\pm$ 231 (4)
Clb3	861 $\pm$ 231 (4)
Clb4	445 $\pm$ 135 (4)
Clb5	784 $\pm$ 193 (5)
Clb6	92 $\pm$ 17 (4)
Sic1	214 $\pm$ 42 (5)
Cdc28	12,263 $\pm$ 3,130 (5)

Extracts from log-phase diploid cultures (W303 background) using the NaOH/TCA method were analyzed for number of copies per cell of the indicated protein fused to protein A, as described in MATERIALS AND METHODS. Note that these are unsynchronized cultures, so the number of copies per cell measured is less than the peak number of copies per cell. Values are mean  $\pm$  SEM, with the number of determinations in parentheses. Figure 4 presents a sample experiment in this series.

difference in protein abundance detected in our experiments. Cln3-associated kinase activity is relatively low under the extraction conditions used by Tyers, and different conditions improve Cln3-associated kinase compared with Cln2 (Jeoung *et al.*, 1998; Miller and Cross, 2000). Tyers *et al.* (1993) did not quantitate their Western signal for Cln3 compared with Cln1 and Cln2, but a value of 7% does not seem unreasonable from inspection of their data. Thus, overall we consider our G1 cyclin quantitation to be in reasonable agreement with published data.

**Table 2.** Cross-check of quantitations using different antibodies and tags

Protein	Antibody	Standard	Copies per diploid cell (asynchronous)
Clb2	Anti-Clb2	MBP-Clb2	2700 $\pm$ 306 (3)
Clb2-protein A	Rabbit IgG	GST-protein A	1128 $\pm$ 231 (4)
Clb5-myc	Anti-myc	GST-myc	1040 $\pm$ 85 (2)
Clb5-protein A	Rabbit IgG	GST-protein A	784 $\pm$ 193 (5)
Cln2-myc	Anti-myc	GST-myc	3250 $\pm$ 636 (2)
Cln2-protein A	Rabbit IgG	GST-protein A	2011 $\pm$ 504 (5)
Cln3-myc	Anti-myc	GST-myc	185 $\pm$ 78 (2)
Cln3-protein A	Rabbit IgG	GST-protein A	216 $\pm$ 44 (6)

All data are derived from diploid strains. The protein A data are reprinted from Table 1 to allow comparison. Experiments determining the level of endogenous Clb2 using anti-Clb2 and MBP-Clb2 as standard, and determining myc-tagged Cln2, Clb5, and Cln3 with GST-myc using anti-myc and GST-myc as standard are presented. The myc-tagged genes were expressed in heterozygous diploids in the BF264-15D background. For the determinations of myc-tagged protein and endogenous Clb2 levels, one culture (two for Clb2) was extracted with the glass bead/SDS method and one with the NaOH/TCA method. These two methods gave similarly efficient extraction and similar results. Values are mean  $\pm$  SEM, with number of determinations in parentheses.

Grandin and Reed (1993) concluded that Clb3 accounted for about two thirds of the total Cdc28 histone H1 kinase activity in asynchronous cells, based on recovery of Cdc28-associated kinase from a *clb3* deletion mutant. This result is not consistent with our finding that Clb3-PrA is present at less than one third the level of the other Clbs added together and at an even lower level when Cln1 and Cln2 are included (Table 1). This discrepancy might suggest that Clb3-PrA levels are under-reporting true Clb3 levels. Alternatively, the effects reported for the *clb3* deletion mutant (Grandin and Reed, 1993) could be indirect effects of *clb3* deletion on levels of other cyclins, or the Clb3-associated kinase could be unusually active relative to other cyclin-associated Cdc28 kinase because of posttranslational effects. The last explanation is unlikely, although, since using IgG-agarose purification, we recover similar levels of histone H1 kinase activity and similar amounts of PrA-tagged cyclin from cells expressing Clb2-PrA and Clb3-PrA (our unpublished results).

Overall, it appears likely that the data obtained by PrA tagging (Table 1) are reasonably accurate. For purposes of discussion we will take the PrA quantitation literally, although the caveats discussed above (both functional and quantitative) should be kept in mind.

### Correlation between Abundance and Functional Importance in B-type Cyclins

The six B-type cyclins derive by gene duplication from a single ancestor and more recent relationships can be observed. The B-type cyclins can be classed by sequence homology and time of expression in the cell cycle into the *CLB5,6*, *CLB3,4*, and *CLB1,2* pairs (Fitch *et al.*, 1992; Grandin and Reed, 1993; Schwob and Nasmyth, 1993). Recent work (Lynch and Conery, 2000) suggests that some gene duplications may be found in modern genomes simply as a consequence of their recent generation. To evaluate the functional significance of the six *CLB* genes, we performed competition growth experiments between various *clb* gene deletions and wild-type strains. We found that deletion of the three *CLB* genes with the least abundant products, *CLB1*, *CLB4*, and *CLB6*, resulted in no significant selective disadvantage in competition with wild type, whereas deletion of the three *CLB* genes with more abundant products, *CLB2*, *CLB3*, and *CLB5*, yielded clear selective disadvantages (Figure 5). (Note that these selective disadvantages are unlikely to be entirely due to differences in exponential growth rate, based on previous data, but we have not attempted to determine the sources of the disadvantages.) This result suggests that although the three sequence classes are functionally distinct and all maintained by natural selection, one member of each class (satisfyingly, in each case the one expressed at a lower level) may not be under strong selection, at least in vegetative culture in rich medium. It is important to note, although, that *CLB1* and *CLB4* have significant roles in meiosis (Grandin and Reed, 1993; Dahmann and Futcher, 1995), which imposes a distinct selective pressure for their maintenance.

Of the mitotic cyclins *CLB1,2,3,4*, *clb2* deletion alone results in a significant cell cycle delay before mitosis, with consequent cell enlargement and reduction of length of G1; in contrast, single deletions of other mitotic *CLB* genes (*CLB1,3,4*) have only minor phenotypes. If these cyclins are fully overlapping in all functional aspects and differ only

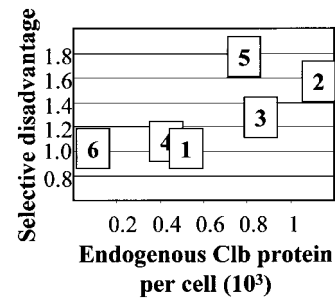


**Figure 5.** Selective disadvantage due to *clb* gene disruption. The selective disadvantage due to the indicated *clb* gene disruption was determined in a single cycle competitive growth experiment from stationary phase, through a dilution of  $\sim 10^6$ -fold, back to stationary phase. The experiment was in liquid YEPD medium, over a 30-h period at 30°C, and the culture initially contained an approximately equal mixture of wild-type and mutant cells. The selective disadvantage parameter will reflect differences in doubling time on the assumption that entry into and exit from stationary phase are identical for all strains, but this has not been tested. In all cases, the *clb* gene disruption was compared with a control strain with identical auxotrophic markers (see MATERIALS AND METHODS).

quantitatively, then the data in Table 1 allow the conclusion that *clb2*-deleted cells should result in a reduction of  $\sim 40\%$  in total mitotic Clb level. This rather moderate reduction can be easily modeled using the Chen *et al.* (2000) parameters by lowering Clb2 synthesis parameters *ksb2'* and *ksb2''* by 40%, yielding about a 12% increase in predicted cell volume at cell division. This increase is significantly less than is observed with *clb2* deletion (Surana *et al.*, 1991). These quantitative considerations may suggest only partial functional overlap among the mitotic cyclins. For example, suppose Clb1 completely overlaps in function with Clb2 (consistent with the high sequence conservation between Clb1 and Clb2), whereas other cyclins are not considered at all. Then the *clb2* deletion will result in about a 70% decrease in Clb1/2 functional protein, which is predicted by the model to yield a nearly twofold increase in cell volume at cell division. An increase of this magnitude is more consistent with observation (Surana *et al.*, 1991). Simple quantitative considerations of this sort may therefore have implications for cyclin functional specificity (see DISCUSSION).

### Abundance through the Cell Cycle and the Role of *Cdh1*

To analyze fluctuations of the PrA-tagged cyclins through the cell cycle, we separated cells on the basis of cell size. In this elutriation method, cultures growing rapidly in rich medium are quickly chilled and then directly fractionated, such that no further physiological response of the culture is required after chilling (Levine *et al.*, 1996; Oehlen *et al.*, 1996). The entire culture is recovered and analyzed in this way. The strategy and sample data are shown in Figure 6A.

This elutriation method loses resolution in the larger size cell fractions. This is in part due to loss of accuracy of size resolution in the fractions containing larger cells, which is evident from a somewhat variable increase in the peak

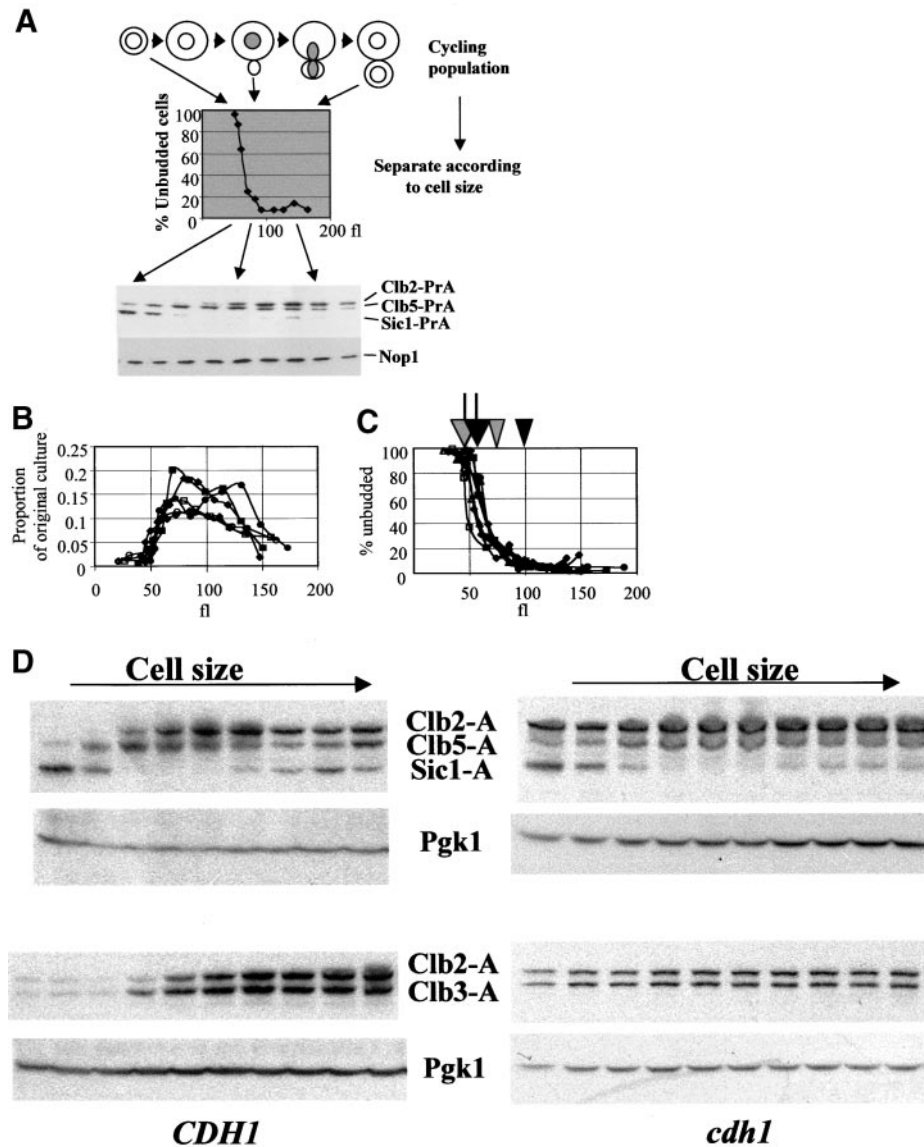


**Figure 6.** Characterization of the elutriation protocol. Log phase cultures of diploid strains heterozygous for various PrA-tagged genes were elutriated as described in MATERIALS AND METHODS. The entire culture was collected. (A) Schematic of the procedure, and sample immunoblotting data. Top: cartoon of an asynchronous population. Middle: the effect of separation on the elutriator, indicated by percentage of unbudded cells. Bottom: sample blot for detection of Clb2-PrA, Clb5-PrA, and Sic1-PrA (all expressed from heterozygous PrA-tagged genes in the diploid strain analyzed). Nop1: loading control detected with anti-Nop1 antibody. (B) The proportion of the total mass of the culture (indicated by  $OD_{660}$ ) as a function of the modal cell volume of the fractions determined by Coulter Channelyzer calibrated with standard 68 fl latex beads. Closed symbols: wild-type diploid strains; open symbols: *cdh1* diploid strains. Each symbol represents a different elutriation. The *cdh1* strains reproducibly yielded significant mass at slightly smaller cell volume than the wild type. In the first few fractions derived from the *cdh1* mutant cultures, two peaks were reproducibly observed in the Coulter Channelyzer electronic cell volume analysis. We do not know the meaning of this observation. For the data reported in Figures 6, B and C, and 7 A and C, we use the larger peak for the *x*-axis values for these samples. (C) The percentage of unbudded cells in the fractions. Closed symbols: wild-type diploid strains; open symbols: *cdh1* diploid strains. Each symbol represents a different elutriation. Arrows above: approximate positions of 50% completion of DNA replication in wild-type (black) and *cdh1* (gray) strains, based on FACS analysis of the fractions. Arrowheads above: beginning of nuclear division,

indicated by initial accumulation of a significant population of binucleate cells, determined by microscopic examination of propidium iodide-stained cells; in earlier fractions, essentially no binucleate cells are observed. (D) PrA detection from diploids doubly heterozygous for *CLB2-PrA*, *CLB5-PrA*, and *SIC1-PrA* (top) or for *CLB2-PrA* and *CLB3-PrA* (bottom). Both *CDH1* (left) and *cdh1* (right) diploids were analyzed. Pgk1 was detected using anti-Pgk1 antibody for a loading control. U, extract from untagged culture. Note that densities of exposure are not comparable between experiments.

width in electronic cell volume measurements (normalized to peak position) for later fractions (our unpublished data). It is also possible that cell size does not correlate as tightly with later cell cycle events. The largest fractions contain cells that have started the next cell cycle before cell separation is complete, as evidenced microscopically by occasional rebudding of already budded cells (our unpublished data). Similarly, FACS analysis shows that the fractions of modal cell volume > 125 fl contain a significant 1C DNA content population upon resonication.

Thus, this method gives an accurate separation of cells in early periods of the cell cycle, from birth until after DNA replication. Fractions with the largest cell sizes (>150 fl) are closer to being asynchronous averages due to loss of resolution of the elutriation.

Multiple diploid strains were analyzed with similar volume distributions and dependence of budding on cell volume (Figure 6, B and C). *cdh1* mutant diploid strains reproducibly budded and initiated DNA replication at ~10 fl smaller volume than the wild type (arrows in Figure 6C) and initiated nuclear division at ~25 fl smaller than wild type (arrowheads

in Figure 6C). An increase in the population of anaphase *cdh1* mutants was noted previously (Visintin *et al.*, 1998).

We elutriated a triply heterozygous diploid, in which coding sequences for Clb2, Clb5 and Sic1 were tagged with PrA on one of the two alleles of each. This allowed a direct comparison of the abundance of the three proteins with the same tag, within the same experiment. We express the units in this experiment relative to peak Clb2 concentration. If peak Clb2 expression corresponds to two times the average asynchronous level (Table 1), one unit on these graphs should correspond to  $\sim 35$  nM (2400 copies/120 fl cell).

As a cross-check, it is possible to predict asynchronous levels of the tagged proteins by integrating across the elutriation profile, multiplying the observed amount of the protein in the size fractions (Figure 7, A and C) by the proportion of the mass of the culture recovered in these fractions (Figure 6A). This can then be compared with the levels directly obtained in asynchronous cells (Table 1). This calculation from the two elutriations quantitated in Figure 7 yields predicted asynchronous Clb2:Clb3:Clb5:Sic1 ratios of 1:0.91:0.91:0.27, compared with ratios from Table 1 of 1:0.76:0.70:0.19. This agreement suggests that the quantitation of the elutriation is reasonably accurate, with most of the proteins recovered and assigned to the different cell size classes.

Although Sic1 was found at quite low levels in asynchronous culture (Table 1), it was abundant in the smallest cells in the culture, where it was in molar excess over the levels of Clb5 and Clb2 coexpressed in the same cells (Figures 6, A and D, and 7A). These cells contributed a very small proportion of the total mass of the culture (Figure 6B), and this could account for the low relative yield of Sic1 in asynchronous total culture (Table 1). If Sic1 inhibits Clb-Cdc28 complexes in a 1:1 stoichiometric ratio, this suggests that under these growth conditions Sic1 is only present at levels sufficient for Clb inhibition for a brief period early in the cell cycle. The onset of DNA replication in cells of  $\sim 60$  fl (black arrow, Figure 6C) correlates with the increase of Clb5 above the Sic1 threshold (Figure 7A). We find that limiting the growth rate of the culture by changing the carbon source from glucose to glycerol increases the duration of the period when Sic1-PrA is high. Thus, growth limitation may expand the high Sic1 pre-Start period of the cell cycle (M.K. and F.C., unpublished data). This expansion is expected based on the known mechanisms for coordinating growth and division in yeast (Hartwell and Unger, 1977; Cross *et al.*, 1989; Cross, 1995).

By comparison with coexpressed cyclins, it appears that the highest concentration of Sic1 found in the smallest cells analyzed is  $\sim 0.4$  times the peak concentration of Clb2 (Figure 7A). Clb2 peaks in the vicinity of 2400 copies per cell (estimating that peak concentration is two times the average concentration reported in Table 1), in cells of  $\sim 120$  fl (Figure 7A), yielding a concentration of 35 nM. Thus, peak Sic1 concentrations should be  $\sim 15$  nM. The  $K_i$  determined for purified Sic1 on Clb-Cdc28 kinase activity was 1.6 nM (Mendenhall, 1993). This will allow Sic1 to be effective at inhibiting Clb kinase, provided there is even a moderate excess of Sic1 over Clbs (assuming 1:1 stoichiometry for inhibition). This effect becomes much stronger if Sic1 is concentrated in the nucleus, but we are unaware of data on this point.

The Chen *et al.* (2000) model predicts qualitatively patterns of accumulation of these different proteins similar to

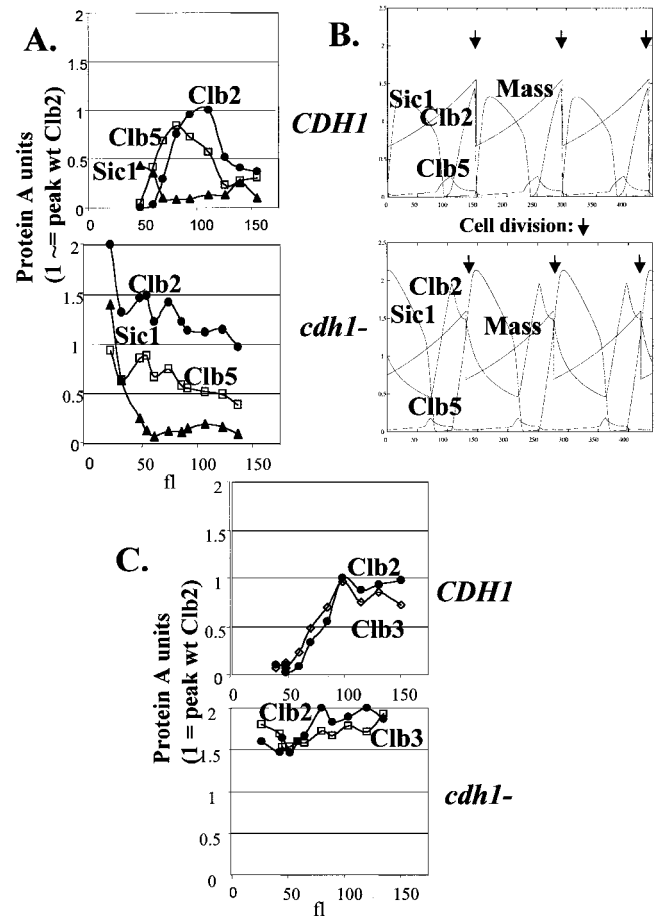


**Figure 7.** Abundance of Clb2, Clb3, Clb5, and Sic1 through the cell cycle, with and without Cdh1: model and experiment. (A) Quantitation of data from Figure 6D, top; diploids heterozygous for *CLB2-PrA*, *CLB5-PrA*, and *SIC1-PrA*. Top: wild type; bottom: *cdh1*. Levels of the PrA fusions were determined densitometrically, and corrected for loading by quantitation of anti-Pgk1 signal. The scale was normalized to 1 for peak Clb2 levels in wild-type cells; this is probably  $\sim 35$  nM (see text). This scale was transferred to the *cdh1* case by comparing a sample with peak Clb2-PrA from a wild-type diploid to a similar sample from a *cdh1* diploid and standardizing the PrA signal to the Pgk1 signal, resulting in the determination that the peak in the *cdh1* mutant was  $\sim 2$  times that in the wild type. This correction is somewhat approximate, compared with the scale within an elutriation, which is internally controlled because of co-expression of single chromosomal identically tagged genes. (B) Model predictions for the levels of the same proteins. Wild type: standard parameters (Chen *et al.*, 2000). *cdh1*: the parameter *kdb2'* was reduced from 2 to 0.01. Mass is total cell mass in the simulation. Arrows indicate cell division. (C) Quantitation of data from Figure 6D, bottom; diploids doubly heterozygous for *CLB2-PrA* and *CLB3-PrA*. Top: wild type; bottom: *cdh1* mutant. Analysis as in A.

what we observe, with several potentially significant differences (Figure 7B). First, the model predicts a long period of time when Sic1 accumulates stably. We observe, in contrast, very little Sic1 accumulating, for only a short time (translating cell volume increments into time, based on the fact that yeast cells probably increase approximately exponentially in

cell mass throughout the cell cycle; Elliott and McLaughlin, 1979). Second, the model calls for a high level of Clb2 compared with Clb5, although we observe nearly comparable levels of these cyclins. Third, Clb2 accumulation appears significantly “peakier” in the model than in the experiment, but this could be a consequence of the poor synchrony in the larger-cell fractions noted above. Overall, the model clearly does a very good job of qualitatively predicting times of accumulation, but the lack of common-scale quantitative information prevented relative levels of different components from being appropriately specified. The more accurate numbers provided here will have consequences for the predicted efficiency with which different cyclins carry out different tasks (see DISCUSSION).

Cdh1 is known to be important for restricting Clb2 protein accumulation, especially in postmitotic cells (Schwab *et al.*, 1997; Visintin *et al.*, 1998; Zachariae *et al.*, 1998). We elutriated a *cdh1* strain triply heterozygous for PrA-tagged *CLB2*, *CLB5*, and *SIC1* genes and found strong deregulation of Clb2 accumulation, with only minor effects on Clb5 and Sic1 accumulation. (The minor fluctuations in Clb2 levels that we observe are not very reproducible; cf. Figure 7A with 7C). It was notable in this background that even in the smallest cells that we could isolate, Sic1 was most likely not in stoichiometric excess over Clb cyclins (because it was not even in clear excess of Clb2 considered alone, without including Clb5, Clb3, and other cyclins). Thus, in the absence of Cdh1, Sic1 regulation of Clb kinase in postmitotic cells may be inefficient. This may account for the entry into DNA replication of these strains at a smaller cell size (gray arrow, Figure 6C).

We approximately standardized the scale of the *cdh1* experiments to the *CDH1* experiments by determining that the signal from peak Clb2 levels in *cdh1* strains was about two times the level in a *CDH1* strain. Thus, all the graphs in Figure 7, A and C, are similarly scaled to a value of 1 for peak Clb2 expression in a *CDH1* strain. (Note that this is an approximation to allow rough quantitative comparison between the experiments and is intrinsically less accurate than the within-experiment comparisons, which are standardized by coexpression of PrA-tagged genes within the same cell.)

The effects of *cdh1* deletion are generally similar to those predicted by the model (Figure 7B), except that a more significant residual regulation of Clb2 is predicted than we observe. These oscillations are predicted because the model assumes very strong transcriptional positive feedback for *CLB2* and cyclical degradation of Clb2 by Cdc20. Both of these ideas are supported by experimental data (Amon *et al.*, 1993; Baumer *et al.*, 2000; Yeong *et al.*, 2000), but the strength of one or both of the effects may be overstated in the model. Alternatively, if Cdc20-dependent Clb2 degradation becomes ineffective at low Clb2 levels (Yeong *et al.*, 2000), detection of *cdh1*-independent degradation could be quite difficult at normal Clb2 expression levels. It will be interesting to implement the proposed biphasic Clb2 degradation (Cdc20-dependent degradation to an intermediate level, followed by Cdh1-dependent degradation; Yeong *et al.*, 2000) in a computational model (see DISCUSSION).

The model predicts oscillations of Clb5 and Sic1 in the *cdh1* strain that are similar to wild type, essentially as we observe. The Clb5 oscillations are predicted to be of lower

amplitude and those of Sic1 of higher amplitude. These are less than twofold effects, and we are not sure if our data confirm these small changes, especially because of the extra correction involved in putting wild-type and *cdh1* data on a common scale (see above). The Sic1 prediction seems better confirmed than the Clb5 prediction (Figure 7B).

The model does not include the Clb3 cyclin. Clb3 overlaps functionally with both the Clb5/6 S cyclins and the Clb1/2 M cyclins (Fitch *et al.*, 1992; Schwob and Nasmyth, 1993) and is also present in asynchronous culture at levels similar to Clb5 and Clb2 (Table 1). We determined the pattern of Clb3 and Clb2 accumulation by elutriating doubly tagged diploid strains and observed similar timing and levels of these two cyclins (Figure 7C). Clb3-PrA reproducibly accumulated in slightly smaller cells than Clb2-PrA, possibly because of earlier transcriptional activation of *CLB3* than *CLB2* (Fitch *et al.*, 1992; Richardson *et al.*, 1992). Grandin and Reed (1993) reported somewhat earlier accumulation of Clb3 than of Clb2. In the experiment in Figure 7C, we did not observe a significant fall-off of Clb2 or Clb3 levels in the largest cells, unlike the results seen in Figure 7A for Clb2; this difference was not reproducible. In experiments (with the same doubly tagged Clb2-PrA, Clb3-PrA strain) where a fall-off of Clb2 was observed in larger cells, a parallel fall-off of Clb3 was also observed (our unpublished data). We attribute the variability to the loss of resolution of the elutriation method in larger cells (see above).

We determined the pattern of accumulation of Clb1-PrA in a diploid doubly heterozygous for tagged *CLB1* and *CLB3*. Clb1 accumulated with periodicity similar to Clb3, but accumulated to only ~60% the peak level of Clb3 (our unpublished results), as expected from the asynchronous values in Table 1.

We observed similar deregulation of both Clb2-PrA and Clb3-PrA by *cdh1* deletion (Figure 7C). This observation suggests that Cdh1 controls both Clb2 and Clb3 accumulation similarly, in disagreement with another report using induced synchrony and overexpressed Clb3 (Baumer *et al.*, 2000). Consistent with our findings, Zachariae *et al.* (1998) showed that ectopic Cdh1 can induce Clb3 degradation, and Alexandru *et al.* (1999) proposed that Clb3 might be under control of both Cdc20 and Cdh1.

### Effects of Constitutive Undegradable Clb2 on Accumulation of Other Cell Cycle Regulators

The model allows explicit predictions to be made about the consequences of interfering with the cell cycle oscillator, not only for cell cycle events but also for accumulation of cell cycle regulators. The availability of a comprehensive set of tagged regulators allows these predictions to be tested. Overexpression of Clb2 lacking its destruction box causes cell cycle arrest late in mitosis (Surana *et al.*, 1993). This genetic manipulation can be simulated in the model (Figure 8A). The model predicts that Clb2-db overexpression should eliminate Cln2, Clb5, and Sic1 proteins. We introduced a *GAL-CLB2-db* cassette or a control *GAL-CLB2* cassette into strains expressing various PrA fusions and tested the effect of a 3.5-h incubation in galactose medium (enough to give efficient cell cycle arrest with *GAL-CLB2-db*). The predicted disappearance of Cln2, Clb5, and Sic1 (Figure 8A) was observed in this experiment (Figure 8B), whereas expression of *GAL-*

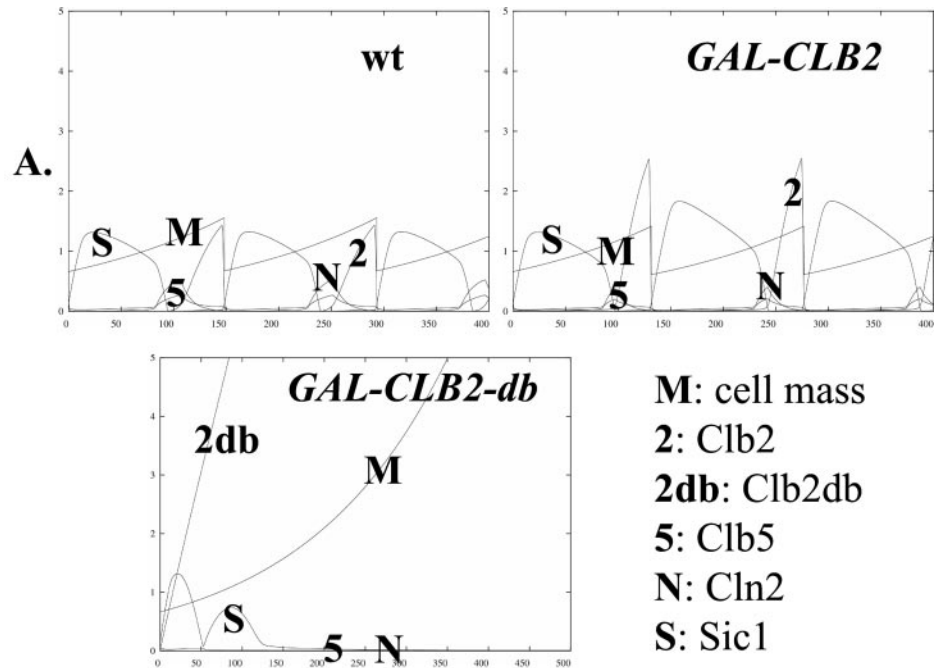
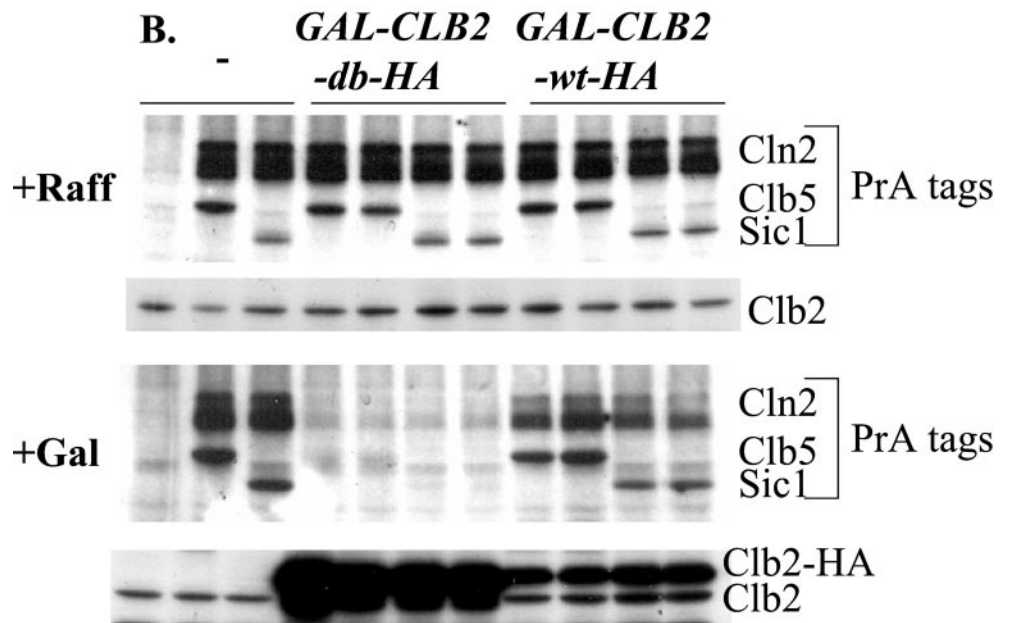


**Figure 8.** Effects of constitutive undegradable Clb2. (A) Model predictions. Loss of transcriptional control of *GAL-CLB2* or *GAL-CLB2db* compared with wild-type *CLB2* was modeled by setting  $ksb2' = 0.05$ ,  $ksb2'' = 0$ . Loss of proteolytic control of *GAL-CLB2db* was modeled by setting  $kdb2''$  to 0.01 and  $kdb2p$  to 0, eliminating degradation dependent on Cdh1 and Cdc20, respectively. (B) Haploid strains expressing the indicated PrA fusions were transformed with integrating plasmids containing *GAL-CLB2-HA* or *GAL-CLB2db-HA* (Jacobson *et al.*, 2000). The untransformed parent and two transformants with each DNA were grown to log phase in YEP-rafinoase (noninducing), and then *GAL-CLB2-HA* or *GAL-CLB2db-HA* was induced by addition of galactose to 3%. After 3.5 h proteins were extracted for PrA detection using rabbit IgG and for Clb2 and Clb2-HA detection using anti-Clb2 antibody.



*CLB2* containing the destruction box was without significant effect, also as the model predicts.

### Effects of Unregulated Cdh1

To examine the effect of making Clb2 degradation constitutive, we constructed strains containing various PrA fusions and also expressing an unregulatable Cdh1 mutant under *GAL* control (*GAL-HA3-HCT1-m11::TRP1*; Zachariae *et al.*, 1998). The galactose-induced mutant Cdh1 protein ex-

pressed from this construct is mutated in its Cdk phosphorylation sites, and so negative control by cyclin-Cdc28 is lost. Thus, this construct results in constitutive Clb2 and Clb3 degradation and blocks the cell cycle (Zachariae *et al.*, 1998). We modeled expression of this construct by simulating Cdh1 not subject to negative regulation by phosphorylation and determined the predicted effects on abundance of Cln2, Clb2, Clb5, and Sic1 (Figure 9A). The model predicts cell cycle arrest with very low levels of Sic1 and Clb2 and very high levels of Cln2 and Clb5. Experimentally, we observed a

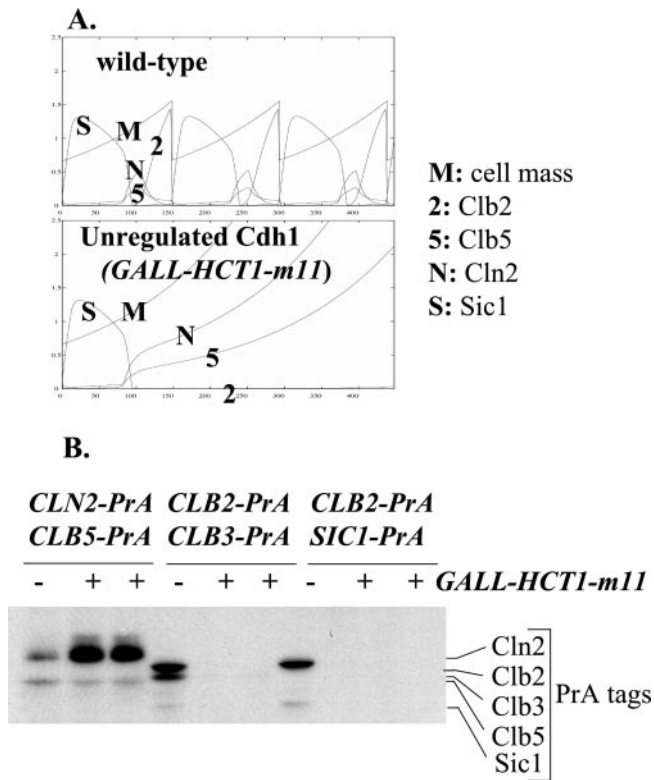


**Figure 9.** Effects of unregulatable Cdh1. (A) Model predictions. Loss of negative regulation of Cdh1 was simulated by setting *kit1* to zero; this simulates prevention of Cdh1 phosphorylation by all cyclin-Cdc28 complexes. (B) Diploid strains were constructed that were heterozygous for the indicated PrA fusions. For each set of fusions, two diploids (+) were also heterozygous for a double integration of the *GALL-HA-HCT1-m11* construct (Zachariae *et al.*, 1998), and one diploid lacked the *GALL-HA-HCT1-m11* construct (-), as indicated. *GALL-HCT1-m11* encodes a mutant Cdh1 (also called Hct1), lacking all Cdk phosphorylation sites and therefore immune to negative regulation (Zachariae *et al.*, 1998). Strains were grown to log phase in YEP-rafinosose (noninducing), and then *GALL-HA-HCT1-m11* was induced by addition of galactose to 3%. After 2.5 h proteins were extracted for PrA detection using rabbit IgG. The band in the approximate position of Sic1-PrA in the strain expressing Clb2-PrA and Clb3-PrA is a Clb3-PrA breakdown product. Quantitation of the Cln2-PrA signal (quantitation of an anonymous cross-reacting band from elsewhere in the gel provided a loading control) indicated a three- to fourfold increase in Cln2-PrA and about a 40% decrease in Clb5-PrA, due to induction of *GALL-HA-HCT1-m11*.

three- to fourfold increase in Cln2-PrA and disappearance of Clb2-PrA and Sic1-PrA, all in accordance with the model's predictions (Figure 9B). We observed no significant increase in Clb5-PrA, in disagreement with the model, but in agreement with previously published data (Schwab *et al.*, 1997; Zachariae *et al.*, 1998).

In this experiment, the effects of unregulated mutant Cdh1 (*GALL-HA3-HCT1-m11*) on Clb2 are likely to be primarily due to direct promotion of Clb2 ubiquitination (leading to its degradation) by Cdh1 (Zachariae *et al.*, 1998). The effects of the mutant Cdh1 on Cln2 and Sic1, in contrast, are likely to be indirect. In the model, unregulated Cdh1 leads to Cln2

accumulation through (1) loss of Clb2, with consequent loss of repression of *CLN2* transcription, leading to (2) hyperaccumulation of Cln2. The hyperaccumulated Cln2 contributes to very efficient Sic1 phosphorylation and SCF-dependent ubiquitination, leading to Sic1 proteolysis.

The incorrectly predicted strong increase in Clb5-PrA by unregulated Cdh1 is also an indirect effect in the model and is predicted for two reasons. First, the model implements Clb2-dependent stimulation of Cdc20 synthesis (Prinz *et al.*, 1998), and Cdc20 is required for efficient Clb5 proteolysis in the model. Second, the model assumes that Clb2 is required to turn off *CLB5* transcription in the same way as it is required to turn off *CLN2* transcription. These two hypothetical mechanisms will make removal of Clb2 by unregulated Cdh1 lead to increased Clb5 levels. There is some information supporting the first assumption (Prinz *et al.*, 1998), but the second assumption is probably incorrect (Amon *et al.*, 1993), as indeed was noted by Chen *et al.* (2000).

We observed a strong reduction in Clb3-PrA levels upon expression of unregulated Cdh1, consistent with the results of Zachariae *et al.* (1998), although the reduction was not as effective as the reduction in Clb2-PrA or Sic1-PrA (with longer exposures, in several experiments; our unpublished data).

Thus, for Cln2, Clb2, and Clb3, we observe opposing effects of *cdh1* deletion (lowering Cln2 and increasing Clb2 and Clb3) and expression of unregulated Cdh1 (increasing Cln2, and strongly reducing Clb2 and Clb3).

## DISCUSSION

### Mathematical Modeling of the Cell Cycle

We report empirical tests of the Chen *et al.* (2000) model for the yeast cell cycle, using genetic and biochemical data not included in the initial model generation. Prediction of dependence of cell size on *CLN3* gene dosage and prediction of cyclin and Sic1 abundance in various situations were reasonably accurate. However, the model gave entirely inaccurate predictions concerning interactions between Cdh1 and G1 cyclins. Possible resolutions are discussed in the next section.

The comprehensive set of tagged regulators that we have constructed here will allow tests of quantitative predictions from the model about these levels of these regulators in cycling cultures and at various oscillator blocks (as in Figures 7–9), providing stringent constraints for evaluation of future models.

Of the cyclins not included in the model, *CLB3* is a good candidate for inclusion in future. Its functional significance is shown by studies of multiple *clb* deletion phenotypes (Fitch *et al.*, 1992; Schwob and Nasmyth, 1993), and single *clb3* deletion results in a significant selective disadvantage (Figure 5). A difficulty in modeling it is that although its transcription is cell cycle regulated (Fitch *et al.*, 1992; Richardson *et al.*, 1992), nothing is known about the mechanism of this regulation.

### Cdh1, Cdc20, and the Control of Clb2 Proteolysis

One way to modify the model to remedy the incorrect predictions on *cdh1* (Figure 3) is to propose increased Cdc20-dependent Clb2 degradation. The current model may have

an excessive reliance on regulated Cdh1 activity to drive the switch from the high-Clb S/M to the low-Clb G1 state. Regulated Cdh1 may function primarily in maintenance rather than initiation of the low-Clb state, and Cdc20 may be important in removal of Clb's at the end of the cell cycle (Baumer *et al.*, 2000; Yeong *et al.*, 2000). Although we observe little regulation of Clb2 accumulation in *cdh1* mutants (Figure 7C), Cdc20 might effectively mediate Clb2 degradation only at higher levels of Clb2 (Yeong *et al.*, 2000). Cdh1 may be required for Clb2 degradation at lower levels. Cdc20-dependent degradation of higher levels of Clb2 might be rapid enough to justify a significant increase in the Chen model's rate constant for Cdc20-dependent Clb2 degradation ( $k_{db2p}$ ), but the proposed loss of this rapid Cdc20-dependent degradation as Clb2 levels decline to lower levels (Yeong *et al.*, 2000) would make Cdh1-independent Clb2 degradation hard to detect using the elutriation approach in Figures 6 and 7.

As noted in the INTRODUCTION, checkpoint/surveillance mechanisms are used in the Chen model to introduce oscillations in Cdc20 activity, in an unperturbed cell cycle. We have found, however, that all DNA- and spindle-dependent surveillance mechanisms can be disabled simultaneously (by constructing *mad1 bub2 mec1 sml1* quadruple mutants) with no significant effects on viability or growth rate (our unpublished data). The checkpoint mechanisms in the model are essentially a way to provide a delay mechanism between initial Clb2 activation and ultimate resulting Cdc20 activation. This is because lifting the checkpoint is dependent on the SPN variable (simulating spindle morphogenesis) reaching a critical value; SPN is under positive control of Clb2, but if the checkpoints do not regulate Cdc20 in unperturbed cell cycles, a revised model might require another way to provide a delay between Clb2 activation and Cdc20 activation.

Clb2 may activate the Cdc20-dependent form of the APC by phosphorylation of APC subunits (Rudner and Murray, 2000). If this activation proceeded with ultrasensitive switch kinetics (Goldbeter and Koshland, 1982), this would provide a checkpoint-independent delay between Clb2 activation and Cdc20 activation. Such kinetics might also account for the proposed biphasic kinetics of Clb2 proteolysis (Yeong *et al.*, 2000). As Clb2 levels fell because of Cdc20-dependent degradation, at some point Clb2 would pass below the levels required to flip the switch, and this could end the Cdc20-dependent phase of Clb2 degradation, if APC phosphorylation were rapidly reversed. Other ideas could also account for the biphasic kinetics (e.g., a fraction of Clb2 might be protected by an unidentified binding partner; Irniger *et al.*, 1995). More genetic and biochemical data is required to accurately implement biphasic Clb2 degradation in a realistic cell cycle control model.

### Cyclin Abundance, Functional Specificity, and $\epsilon$ Factors

Deletions of the different cyclin genes have distinct consequences. The simplest way this could happen is if one cyclin is the most abundant; its deletion might then be expected to have the most severe consequences. For the mitotic B-type cyclins *CLB1,2,3,4*, the order of severity of phenotypes from deletion analysis (Surana *et al.*, 1991; Fitch *et al.*, 1992) indicates that Clb2 is the most important. *clb2* deletion is the

only single-*CLB* deletion in this set with a recognizable phenotype, and all multiple deletion combinations that are lethal or semilethal include *clb2*. Following *CLB2* in importance are *CLB1* and *CLB3*, because *clb1 clb2* and *clb2 clb3* double mutants are semilethal. *CLB4* appears to be of minor importance. The order of importance of Clb1,2,3,4 from these genetic studies:  $2 > 1,3 > 4$ , follows the order of their calculated abundance (Table 1). Determination of selective disadvantage due to *clb* deficiencies (Figure 5) confirms that only the more abundant ones have a phenotype detectable by this assay. Thus, some apparent cyclin specificity may be due simply to relative abundance. As discussed above, this factor seems unlikely to explain all the data even among these mitotic cyclins, and it is clear that relative abundance cannot universally explain cyclin specificity (reviewed in Miller and Cross, 2001). Instead, some cyclins must be intrinsically specialized, independent of abundance or timing of expression.

To reflect this idea of intrinsic cyclin specialization, Chen *et al.* (2000) use  $\epsilon$  factors to state the efficiency of a given cyclin for a given cell cycle task. With respect to phosphorylation of Sic1 by cyclin-Cdc28, both Cln2- and Clb2-complexes can phosphorylate Sic1 in vitro with broadly similar efficiency (Verma *et al.*, 1997b), although Clb5-Cdc28 may be less effective than Cln2-Cdc28 (Elsasser *et al.*, 1999). The  $\epsilon$  factors in the model do not reflect these findings ( $\epsilon$  factors for Sic1 inactivation of 1, 1, 0.067 for Cln2, Clb5, and Clb2, respectively). No large differences in Cdh1 phosphorylation in vitro by various Clb complexes were noted (Zachariae *et al.*, 1998), and genetic data suggests that Clb5 may be better than Clb2 at inducing Cdh1 phosphorylation (Shirayama *et al.*, 1999). In contrast, the model parameters suggest twofold more efficient phosphorylation of Cdh1 by Clb2 complexes than by Clb5 complexes.

Genetic experiments where expression and timing of different cyclins have been equalized indicate strong differences in efficiency for inducing DNA replication or for inhibiting mitotic exit for Clb5 versus Clb2 (Cross *et al.*, 1999; Jacobson *et al.*, 2000), whereas both Clb2 and Clb5 appear able to inhibit reloading of replication origins (Nasmyth, 1996; Jacobson *et al.*, 2000). Similar experiments indicate sharp differences in ability to promote various Start-related events for Cln3 versus Cln2 (Levine *et al.*, 1996; e.g., Cln3 is better able to activate SBF-mediated transcription; Cln2 is better at driving bud emergence). These differences in efficiency between Clb2 and Clb5 and between Cln2 and Cln3 are reflected in the model parameters.

### Interpreting the Quantitations: How Much is a Lot?

To fully interpret our quantitations (Table 1), subcellular localization must be determined. For example, the model (Chen *et al.*, 2000) proposes a 75-fold greater efficiency of Cln3 compared with Cln1 or Cln2 for activating SBF-regulated transcription. In a compartmentalized model, this extreme efficiency difference may be an unnecessary factor, despite the lower overall cellular concentration of Cln3 compared with Cln1 and Cln2 (Table 1). If Cln2 is uniformly distributed through the cell or excluded from the nucleus, and Cln3 is nuclear-restricted (Miller and Cross, 2000), Cln3 might be at least 2.7-fold more concentrated in the nucleus than Cln2. (216 copies Cln3/4 fl nucleus/2011 copies Cln2/

100 fl cell = 2.7, assuming a 4-fl diploid nucleus in a 100-fl cell, because a haploid nucleus is  $\sim 2$  fl; Winey *et al.*, 1997).

One of the main roles of Clb5 is to activate DNA replication (Epstein and Cross, 1992; Schwob and Nasmyth, 1993; Donaldson *et al.*, 1998). Clb5 is concentrated in the nucleus (Shirayama *et al.*, 1999; Jacobson *et al.*, 2000). An asynchronous average of 800 copies per diploid cell (Table 1) yields a peak nuclear concentration around 1  $\mu$ M or 2400 per nucleus, assuming a threefold enrichment at peak over average. Eight percent of the yeast haploid genome contains about 48 origins (Poloumienko *et al.*, 2001), yielding an estimated 1100 origins per diploid genome; similarly, Orc2 (which binds to replication origins as part of the essential ORC complex) was quantitated at  $\sim 600$  copies per haploid cell (Donovan *et al.*, 1997). Thus, Clb5-origin affinity may not need to be very high, because Clb5 nuclear concentration is high and Clb5 may be in stoichiometric excess over origins ( $2400/1110 = 2$  Clb5/origin).

In addition to activating replication origin firing, Clb kinases also prevent reloading of replication origins, and this is proposed to contribute to once-per-cell-cycle control of DNA replication (Nasmyth, 1996). Targets for Cdc28-dependent phosphorylation for negative control of replication include Cdc6, the Mcm2–7 complex, and the Orc complex (Nguyen *et al.*, 2001). The abundance of the Orc complex is likely to be similar to that of replication origins (see above), so Clb kinases (considered jointly) are probably significantly more abundant than the Orc complex targets at all times after DNA replication is completed. The Mcm complex may be as much as 50-fold more abundant than the Orc complex (Donovan *et al.*, 1997), so efficient phosphorylation of the Mcm complex may require a more efficient interaction with Clb kinases. Alternatively, since phosphorylation leads to nuclear export of the Mcm complex (Nguyen *et al.*, 2000), even relatively inefficient phosphorylation of the Mcm complex could eventually drain the complex from the nucleus, assuming the Clb kinases remain nuclear.

Cln2 accumulates to a level greater than Sic1 (Table 1). Sic1 is a proposed enzymatic target for Cln2-Cdc28 complexes (Schwob *et al.*, 1994; Verma *et al.*, 1997a, 1997b), and these calculations suggest that a high affinity of Cln2-Cdc28 for Sic1 may not be required for effective phosphorylation of Sic1.

It is interesting that none of the calculations above for relative levels of cyclins and phosphorylation targets imply the need for high-affinity interactions between the cyclin and the target. This could have implications for the tightness of interaction required in general between potential substrate-targeting regions in cyclins (e.g., Cross and Jacobson, 2000) and the phosphorylation targets.

The kinase catalytic subunit Cdc28 was detected at higher levels than any cyclin, about 12,000 copies per cell. Cdk's are generally thought to be in excess of cyclins; the level of Cdc28 calculated here, although in excess, is not tremendously so. This could have implications for experiments in which cyclins are overexpressed, since at high cyclin expression levels competition for Cdc28 could become a significant factor.

The apparently low level of Sic1 in measurements from asynchronous culture (Table 1) nevertheless allows for effective inhibition of Clb kinases in small newborn cells, as predicted (Schwob *et al.*, 1994; see RESULTS).

## CONCLUSION

An ideal chemical kinetic model would replace dimensionless concentration terms with molarities in the appropriate subcellular compartment and would replace  $\epsilon$  factors with association, dissociation, and enzymatic rate constants. Although this ideal will not be achieved for cell cycle control in the immediate future, the attempt to meet it will generate testable quantitative hypotheses that might be hard to obtain by intuition. Empirical studies targeted at model testing should allow efficient development of more realistic quantitative models, perhaps ultimately leading to true predictive tools.

## ACKNOWLEDGMENTS

The authors thank Caihong Li for expert technical assistance, especially in the challenging experiment in Figure 1; John Tyson and Kathy Chen for help in understanding and using the model; Mike Rout and Brian Chait for useful discussions; Peter Schwartz and Jung-Im Lee for preliminary work in the system presented in Figure 2; Phillip Kaldis and Mike Rout for plasmids; Angelika Amon, Bruce Futcher, and Masaki Shirayama for strains; and Mike Rout for the anti-Nop1 antibody. This work was supported by Public Health Service grant GM47238.

## REFERENCES

- Aitchison, J., Rout, M., Marelli, M., Blobel, G., and Wozniak, R.W. (1995). Two novel related yeast nucleoporins NUP170p and NUP157p: complementation with the vertebrate homologue NUP155p and functional interactions with the yeast nuclear pore-membrane protein POM152p. *J. Cell Biol.* 131, 1133–1148.
- Alexandru, G., Zachariae, W., Schleiffer, A., and Nasmyth, K. (1999). Sister chromatid separation and chromosome re-duplication are regulated by different mechanisms in response to spindle damage. *EMBO J.* 18, 2707–2721.
- Amon, A., Tyers, M., Futcher, B., and Nasmyth, K. (1993). Mechanisms that help the yeast cell cycle clock tick: G2 cyclins transcriptionally activate G2 cyclins and repress G1 cyclins. *Cell* 74, 993–1007.
- Bardin, A., Visintin, R., and Amon, A. (2000). A mechanism for coupling exit from mitosis to partitioning of the nucleus. *Cell* 102, 21–31.
- Baumer, M., Braus, G., and Irniger, S. (2000). Two different modes of cyclin clb2 proteolysis during mitosis in *Saccharomyces cerevisiae*. *FEBS Lett.* 468, 142–148.
- Chen, K., Csikasz-Nagy, A., Gyorffy, B., Val, J., Novak, B., and Tyson, J. (2000). Kinetic analysis of a molecular model of the budding yeast cell cycle. *Mol. Biol. Cell* 11, 369–391.
- Cross, F., and Jacobson, M. (2000). Conservation and function of a potential substrate-binding domain in the yeast Clb5 B-type cyclin. *Mol. Cell. Biol.* 20, 4782–4790.
- Cross, F., Roberts, J., and Weintraub, H. (1989). Simple and complex cell cycles. *Annu. Rev. Cell Biol.* 5, 341–395.
- Cross, F.R. (1990). Cell cycle arrest caused by *CLN* gene deficiency in *Saccharomyces cerevisiae* resembles START-I arrest and is independent of the mating-pheromone signaling pathway. *Mol. Cell. Biol.* 10, 6482–6490.
- Cross, F.R. (1988). *DAF1*, a mutant gene affecting size control, pheromone arrest, and cell cycle kinetics of *Saccharomyces cerevisiae*. *Mol. Cell Biol.* 8, 4675–4684.

- Cross, F.R. (1989). Further characterization of a size control gene in *Saccharomyces cerevisiae*. *J. Cell Sci.* 94(Suppl 12), 117–127.
- Cross, F.R. (1995). Starting the cell cycle: what's the point? *Curr. Opin. Cell Biol.* 7, 790–797.
- Cross, F.R., and Blake, C.M. (1993). The yeast Cln3 protein is an unstable activator of Cdc28. *Mol. Cell Biol.* 13, 3266–3271.
- Cross, F.R., Yuste-Rojas, M., Gray, S., and Jacobson, M. (1999). Specialization and targeting of B-type cyclins. *Mol. Cell* 4, 11–19.
- Dahmann, C., and Futcher, B. (1995). Specialization of B-type cyclins for mitosis or meiosis in *S. cerevisiae*. *Genetics* 140, 957–963.
- Di Como, C.J., Chang, H., and Arndt, K.T. (1995). Activation of *CLN1* and *CLN2* G1 cyclin gene expression by BCK2. *Mol. Cell Biol.* 15, 1835–1846.
- Donaldson, A.D., Raghuraman, M.K., Friedman, K.L., Cross, F.R., Brewer, B.J., and Fangman, W.L. (1998). CLB5-dependent activation of late replication origins in *S. cerevisiae*. *Mol. Cell* 2(2), 173–182.
- Donovan, S., Harwood, J., Drury, L.S., Diffley, J.F. (1997). Cdc6p-dependent loading of Mcm proteins onto prereplicative chromatin in budding yeast. *Proc Natl Acad Sci USA.* 27, 5611–5616.
- Elliott, S., and McLaughlin, C. (1979). Synthesis and modification of proteins during the cell cycle of the yeast *Saccharomyces cerevisiae*. *J. Bacteriol.* 137, 1185–1190.
- Elsasser, S., Chi, Y., Yang, P., and Campbell, J. (1999). Phosphorylation controls timing of Cdc6p destruction: A biochemical analysis. *Mol. Biol. Cell* 10, 3263–3277.
- Epstein, C.B., and Cross, F.R. (1992). *CLB5*: A novel B cyclin from budding yeast with a role in S phase. *Genes Dev.* 6, 1695–1706.
- Epstein, C.B., and Cross, F.R. (1994). Genes that can bypass the *CLN* requirement for *Saccharomyces cerevisiae* cell cycle START. *Mol. Cell Biol.* 14, 2041–2047.
- Fitch, I., Dahmann, C., Surana, U., Amon, A., Nasmyth, K., Goetsch, L., Byers, B., and Futcher, B. (1992). Characterization of four B-type cyclin genes of the budding yeast *Saccharomyces cerevisiae*. *Mol. Biol. Cell* 3, 805–818.
- Funakoshi, M., Sikder, H., Ebihara, H., Irie, K., Sugimoto, K., Matsumoto, K., Hunt, T.N., T, and Kobayashi, H. (1997). *Xenopus* cyclin A1 can associate with Cdc28 in budding yeast, causing cell-cycle arrest with an abnormal distribution of nuclear DNA. *Genes Cells* 2, 329–43.
- Goldbeter, A., and Koshland, D.E., Jr. (1981). An amplified sensitivity arising from covalent modification in biological systems. *Proc. Natl. Acad. Sci. USA* 78, 6840–6844.
- Grandin, N., and Reed, S.I. (1993). Differential function and expression of *Saccharomyces cerevisiae* B-type cyclins in mitosis and meiosis. *Mol. Cell Biol.* 13, 2113–2125.
- Haase, S., Winey, M., and Reed, S. (2001). Multi-step control of spindle pole body duplication by cyclin-dependent kinase. *Nat. Cell Biol.* 3, 38–42.
- Hartwell, L.H., and Unger, M.W. (1977). Unequal division in *Saccharomyces cerevisiae* and its implications for the control of cell division. *J. Cell Biol.* 75, 422–435.
- Holm, C., Meeks-Wagner, D.W., Fangman, W.L., and Botstein, D. (1986). A rapid, efficient method for isolating DNA from yeast. *Gene* 42, 169–173.
- Irniger, S., Piatti, S., Michaelis, C., and Nasmyth, K. (1995). Genes involved in sister chromatid separation are needed for B-type cyclin proteolysis in budding yeast. *Cell.* 81, 269–278.
- Irniger, S., and Nasmyth, K. (1997). The anaphase promoting complex is required in G1 arrested cells to inhibit B-type cyclin accumulation and to prevent uncontrolled entry into S phase. *J. Cell Sci.* 110, 1523–1531.
- Jacobson, M.D., Gray, S., Yuste-Rojas, M., and Cross, F.R. (2000). Testing cyclin specificity in the exit from mitosis. *Mol. Cell Biol.* 20, 4483–93.
- Jaspersen, S., Charles, J., and Morgan, D. (1999). Inhibitory phosphorylation of the APC regulator Hct1 is controlled by the kinase Cdc28 and the phosphatase Cdc14. *Curr. Biol.* 9, 227–236.
- Jaspersen, S., Charles, J., Tinker-Kulberg, R., and Morgan, D. (1998). A late mitotic regulatory network controlling cyclin destruction in *Saccharomyces cerevisiae*. *Mol. Biol. Cell* 9, 2803–2817.
- Jeoung, D., Oehlen, L.J.W.M., and Cross, F.R. (1998). Cln3-associated kinase activity in *Saccharomyces cerevisiae* is regulated by the mating factor pathway. *Mol. Cell Biol.* 18, 433–441.
- Knapp, D., Bhoite, L., Stillman, D.J., and Nasmyth, K. (1996). The transcription factor Swi5 regulates expression of the cyclin kinase inhibitor p40SIC1. *Mol. Cell Biol.* 16, 5701–5707.
- Koch, C., and Nasmyth, K. (1994). Cell cycle regulated transcription in yeast. *Curr. Opin. Cell Biol.* 6, 451–459.
- Koch, C., Schleiffer, A., Ammerer, G., and Nasmyth, K. (1996). Switching transcription on and off during the yeast cell cycle: Cln/Cdc28 kinases activate bound transcription factor SBF (Swi4/Swi6) at Start, whereas Clb/Cdc28 kinases displace it from the promoter in G2. *Genes Dev.* 10, 129–141.
- Levine, K., Huang, K., and Cross, F.R. (1996). *Saccharomyces cerevisiae* G1 cyclins differ in their intrinsic functional specificities. *Mol. Cell Biol.* 16, 6794–6803.
- Lynch, M., and Conery, J.S. (2000). The evolutionary fate and Consequences of Duplicate Genes. *Science* 290, 1151–1155.
- McInerney, C.J., Partridge, J.F., Mikesell, G.E., Creemer, D.P., and Breeden, L.L. (1997). A novel Mcm1-dependent element in the *SWI4*, *CLN3*, *CDC6*, and *CDC47* promoters activates M/G1-specific transcription. *Genes Dev.* 11, 1277–1288.
- Mendenhall, M.D. (1993). An inhibitor of p34<sup>CDC28</sup> protein kinase activity from *Saccharomyces cerevisiae*. *Science* 259, 216–219.
- Miller, M., and Cross, F.R. (2001). Cyclin specificity: how many wheels do you need for a unicycle? *J. Cell Sci.* 114, 1811–1820.
- Miller, M.E., and Cross, F.R. (2000). Distinct subcellular localization patterns contribute to functional specificity of the Cln2 and Cln3 cyclins of *Saccharomyces cerevisiae*. *Mol. Cell Biol.* 20, 542–555.
- Morgan, D. (1997). Cyclin-dependent kinases: engines, clocks, and microprocessors. *Annu. Rev. Cell. Dev. Biol.* 13, 261–291.
- Nash, R., Tokiwa, G., Anand, S., Erickson, K., and Futcher, A.B. (1988). The *WHI1+* gene of *Saccharomyces cerevisiae* tethers cell division to cell size and is a cyclin homolog. *EMBO J.* 7, 4335–4346.
- Nasmyth, K. (1996). At the heart of the budding yeast cell cycle. *Trends Genet.* 12, 405.
- Nguyen, V.Q., Co, C., Irie, K., and Li, J.J. (2000). Clb/Cdc28 kinases promote nuclear export of the replication initiator proteins Mcm2–7. *Curr. Biol.* 10, 195–205.
- Nguyen, V.Q., Co, C., and Li, J.J. (2001). Cyclin-dependent kinases prevent DNA re-replication through multiple mechanisms. *Nature* 411, 1068–1073.
- Novak, B., Csikasz-Nagy, A., Gyorfy, B., Nasmyth, K., and Tyson, J. (1998). Model scenarios for evolution of the eukaryotic cell cycle. *Philos. Trans. R. Soc. Lond. B Biol. Sci.* 353, 2063–2076.
- Oehlen, L.J.W.M., McKinney, J.D., and Cross, F.R. (1996). Ste12 and Mcm1 regulate cell cycle dependent transcription of *FAR1*. *Mol. Cell Biol.* 16, 2830–2837.

- Poloumienko, A., Dershowitz, A., De, J., Newlon, C.S. (2001). Completion of replication map of *Saccharomyces cerevisiae* chromosome III. *Mol Biol Cell*. 12, 3317–3327.
- Prinz, S., Hwang, E., Visintin, R., and Amon, A. (1998). The regulation of Cdc20 proteolysis reveals a role for APC components Cdc23 and Cdc27 during S phase and early mitosis. *Curr. Biol*. 8, 750–760.
- Richardson, H., Lew, D.J., Henze, M., Sugimoto, K., and Reed, S.I. (1992). Cyclin-B homologs in *Saccharomyces cerevisiae* function in S phase and in G<sub>2</sub>. *Genes Dev*. 6, 2021–2034.
- Rudner, A., and Murray, A. (2000). Phosphorylation by Cdc28 activates the Cdc20-dependent activity of the anaphase-promoting complex. *J. Cell Biol*. 149, 1377–1390.
- Schwab, M., Lutum, A.S., and Seufert, W. (1997). Yeast Hct1 is a regulator of Clb2 cyclin proteolysis. *Cell* 90, 683–693.
- Schwob, E., Boehm, T., Mendenhall, M.D., and Nasmyth, K. (1994). The B-type cyclin kinase inhibitor p40SIC1 controls the G1 to S transition in *S. cerevisiae*. *Cell* 79, 233–244.
- Schwob, E., and Nasmyth, K. (1993). *CLB5* and *CLB6*, a new pair of B cyclins involved in DNA replication in *Saccharomyces cerevisiae*. *Genes Dev*. 7, 1160–1175.
- Shirayama, M., Toth, A., Galova, M., and Nasmyth, K. (1999). APC-CDC20 promotes exit from mitosis by destroying the anaphase inhibitor Pds1 and cyclin Clb5. *Nature* 402, 203–207.
- Shou, W., Seol, J., Shevchenko, A., Baskerville, C., Moazed, D., Chen, Z., Jang, J., Shevchenko, A., Charbonneau, H., and Deshaies, R. (1999). Exit from mitosis is triggered by Tem1-dependent release of the protein phosphatase Cdc14 from nucleolar RENT complex. *Cell* 97, 233–244.
- Surana, U., Amon, A., Dowzer, C., McGrew, J., Byers, B., and Nasmyth, K. (1993). Destruction of the CDC28/CLB mitotic kinase is not required for the metaphase to anaphase transition in budding yeast. *EMBO J*. 12, 1969–1978.
- Surana, U., Robitsch, H., Price, C., Schuster, T., Fitch, I., Futcher, A.B., and Nasmyth, K. (1991). The role of CDC28 and cyclins during mitosis in the budding yeast *S. cerevisiae*. *Cell* 65, 145–161.
- Toyn, J.H., Johnson, A.L., Donovan, J.D., Toone, W.M., and Johnston, L.H. (1996). The Swi5 transcription factor of *Saccharomyces cerevisiae* has a role in exit from mitosis through induction of the cdk-inhibitor Sic1 in telophase. *Genetics* 145, 85–96.
- Tyers, M. (1996). The cyclin-dependent kinase inhibitor p40SIC1 imposes the requirement for *CLN* G1 cyclin function at Start. *Proc. Natl. Acad. Sci. USA* 93, 7772–7776.
- Tyers, M., Tokiwa, G., and Futcher, B. (1993). Comparison of the *Saccharomyces cerevisiae* G<sub>1</sub> cyclins: Cln3 may be an upstream activator of Cln1, Cln2 and other cyclins. *EMBO J*. 12, 1955–1968.
- Tyers, M., Tokiwa, G., Nash, R., and Futcher, B. (1992). The Cln3-Cdc28 kinase complex of *S. cerevisiae* is regulated by proteolysis and phosphorylation. *EMBO J*. 11, 1773–1784.
- Vallen, E., and Cross, F. (1999). Interaction between the MEC1-dependent DNA synthesis checkpoint and G1 cyclin function in *Saccharomyces cerevisiae*. *Genetics* 151, 459–471.
- Verma, R., Annan, R.S., Huddleston, M.J., Carr, S.A., Reynard, G., and Deshaies, R.J. (1997a). Phosphorylation of Sic1p by G<sub>1</sub> Cdk required for its degradation and entry into S phase. *Science* 278, 455–460.
- Verma, R., Feldman, R.M.R., and Deshaies, R.J. (1997b). SIC1 is ubiquitinated in vitro by a pathway that requires CDC4, CDC34, and cyclin/CDK activities. *Mol. Biol. Cell* 8, 1427–1437.
- Visintin, R., Craig, K., Hwang, E., Prinz, S., Tyers, M., and Amon, A. (1998). The phosphatase Cdc14 triggers mitotic exit by reversal of Cdk-dependent phosphorylation. *Mol. Cell* 2, 709–718.
- Visintin, R., Hwang, E., and Amon, A. (1999). Cfi1 prevents premature exit from mitosis by anchoring Cdc14 phosphatase in the nucleolus. *Nature* 398, 818–823.
- Visintin, R., Prinz, S., and Amon, A. (1998). *CDC20* and *CDH1*: A family of substrate-specific activators of APC-dependent proteolysis. *Science* 278, 460–463.
- Wach, A., Brachat, A., Alberti-Segui, C., Rebischung, C., and Philippsen, P. (1997). Heterologous HIS3 marker and GFP reporter modules for PCR-targeting in *Saccharomyces cerevisiae*. *Yeast* 13, 1065–1075.
- Winey, M., Yarar, D., Giddings, T.J., and Mastronarde, D. (1997). Nuclear pore complex number and distribution throughout the *Saccharomyces cerevisiae* cell cycle by three-dimensional reconstruction from electron micrographs of nuclear envelopes. *Mol. Biol. Cell* 8, 2119–2132.
- Yeong, F., Lim, H., Padmashree, C., and Surana, U. (2000). Exit from mitosis in budding yeast: biphasic inactivation of the Cdc28-Clb2 mitotic kinase and the role of Cdc20. *Mol. Cell* 5, 501–511.
- Zachariae, W., and Nasmyth, K. (1999). Whose end is destruction: cell division and the anaphase-promoting complex. *Genes Dev*. 15, 2039–2058.
- Zachariae, W., Schwab, M., Nasmyth, K., and Seufert, W. (1998). Control of cyclin ubiquitination by CDK-regulated binding of Hct1 to the anaphase promoting complex. *Science* 282, 1721–1724.
- Zhao, X., Muller, E., and Rothstein, R. (1998). A suppressor of two essential checkpoint genes identifies a novel protein that negatively affects dNTP pools. *Mol. Cell*. 1998 2, 329–340.